Refining the model of barrier island formation along a paraglacial coast in the Gulf of Maine

Christopher J. Hein[a,*], Duncan M. FitzGerald[a], Emily A. Carruthers[b], Byron D. Stone[c], Walter A. Barnhardt[d], Allen M. Gontz[e]

[a] Department of Earth Sciences, Boston University, 675 Commonwealth Ave., Boston, MA 02215, USA. hein@whoi.edu, dunc@bu.edu

[b] Department of Earth Sciences, Boston University; Present Address: Sea Education Association, PO Box 6, Woods Hole, MA 02543, USA. ecarruthers@sea.edu

[c] U.S. Geological Survey, 12201 Sunrise Valley Drive Mail Stop 926A, Reston, VA 20192, USA. bdstone@usgs.gov

[d] U.S. Geological Survey, Woods Hole Coastal Science Center, Woods Hole, MA 02543, USA. wbarnhardt@usgs.gov

[e] Department of Environmental, Earth, and Ocean Sciences, University of Massachusetts, Boston, 100 Morrissey Blvd., Boston, MA 02125, USA. allen.gontz@umb.edu

* - Corresponding author: Present Address: Woods Hole Oceanographic Institution, MS #04, 266 Woods Hole Rd., Woods Hole, MA 02543, USA; Email: hein@whoi.edu; Phone: 001-857-753-3566; Fax: 001-508-457-2164

Highlights

- A new, detailed evolutionary model for the longest barrier in the Gulf of Maine and n updated chronologic framework for Holocene sea-level change and barrier development in northern Massachusetts are presented.
- Spit elongation accounts for more than 60% of the barrier length
- Shoreline progradation accounts for more than 90% of the barrier width
- A paleo-inlet was active in central Plum Island around 3.5–3.6 ka.
- Inlet closure occurred due to backbarrier infilling and tidal prism reduction.

Abstract

Details of the internal architecture and local geochronology of Plum Island, the longest barrier in the Gulf of Maine, has refined our understanding of barrier island formation in paraglacial settings. Ground-penetrating radar and shallow-seismic profiles coupled with sediment cores and radiocarbon dates provide an 8000-year evolutionary history of this barrier system in response to changes in sediment sources and supply rates as well as variability in the rate of sea-level change. The barrier sequence overlies tills of Wisconsinan and Illinoian glaciations as well as late Pleistocene glaciomarine clay deposited during the post-glacial sea-level highstand at approximately 17 ka. Holocene sediment began accumulating at the site of Plum Island at 7–8 ka, in the form of coarse fluvial channel-lag deposits related to the 50-m wide erosional channel of the Parker River that carved into underlying glaciomarine deposits during a lower stand of sea level. Plum Island had first developed in its modern location by ca. 3.6 ka through onshore migration and vertical accretion of reworked regressive and lowstand deposits. The prevalence of southerly, seaward-dipping layers indicates that greater than 60% of the

barrier lithosome developed in its modern location through southerly spit progradation, consistent with a dominantly longshore transport system driven by northeast storms. Thinner sequences of northerly, landward-dipping clinoforms represent the northern recurve of the prograding spit. A 5–6-m thick inlet-fill sequence was identified overlying the lower stand fluvial deposit; its stratigraphy captures events of channel migration, ebb-delta breaching, onshore bar migration, channel shoaling and inlet infilling associated with the migration and eventual closing of the inlet. This inlet had a maximum cross-sectional area of 2800 m^2 and was active around 3.5–3.6 ka. Discovery of this inlet suggests that the tidal prism was once larger than at present. Bay infilling, driven by the import of sediment into the backbarrier environment through tidal inlets, as well as minor sediment contribution from local rivers, led to a vast reduction in the bay tidal prism. This study demonstrates that, prior to about 3 ka, Plum Island and its associated marshes, tidal flats, and inlets were in a paraglacial environment; that is, their main source of sediment was derived from the erosion and reworking of glaciogenic deposits. Since that time, Plum Island has been in a state of dynamic equilibrium with its non-glacial sediment sources and therefore can be largely considered to be in a stable, “post-paraglacial” state. This study is furthermore the first in the Gulf of Maine to show that spit accretion and inlet processes were the dominant mechanisms in barrier island formation and thus serves as a foundation for future investigations of barrier development in response to backbarrier infilling.

Keywords

Inlet processes; Inlet-fill sequence; Spit accretion; Barrier-island formation; Paraglacial; Ground-penetrating radar

1. Introduction

Paraglacial barrier coasts are located in regions formerly covered by ice sheets that still retain an extensive surface cover of easily-erodible glaciogenic sediments. Such coastal landscapes are associated with >30% of Northern Hemisphere continental shelves and are found throughout Northern Europe, Siberia, Iceland, Greenland, the northern coasts of North America, and emerging Arctic coastlines (Forbes and Syvitski, 1994; Forbes, 2005). They are generally dominated by headlands, bays, and pocket beaches (FitzGerald and van Heteren, 1999. Along high-latitude (>45^{o} N), previously-glaciated coasts, barriers are rare and isolated and are composed of coarse-grained sand and gravel (Hayes, 1979; FitzGerald and van Heteren, 1999). By contrast, paraglacial coasts in middle-latitude regions (40–45^{o} N) have been affected by late Pleistocene and early Holocene sea-level changes that have tended to smooth coastal landforms, rework glacial and fluvial deposits and produce barrier islands, mainland-attached barriers, and spits. Nearly 25% of the middle-latitude paraglacial coast of New England (northeast USA) contains barriers (FitzGerald and van Heteren, 1999). They are a dominant coastal feature in much of southern New England and are often located proximal to major rivers. Due to the compartmentalized nature of the beach systems in this region (Kelley, 1987), these barriers generally average only about 1 km in length (Duffy et al., 1989) and are composed of finer-grained sediment (fine- to coarse- sand) than is found in other paraglacial settings (coarse sand to gravel; FitzGerald and van Heteren, 1999).

These New England coasts are typically bedrock-dominated and receive sediment largely from the excavation and reworking of Pleistocene glaciogenic landforms (Forbes and Syvitski, 1994; Ballantyne, 2002). They therefore contain mixed sediments which reflect their various glacial, glacio-marine, glacio-fluvial, fluvial, and shelf sediment sources (FitzGerald and van

Heteren, 1999). The deposition and sustenance of coastal barrier systems along these paraglacial coasts are related not only to their variable glaciogenic sediment sources and supply rates, but also to the lengthy postglacial period (10^3-10^4 yrs) of complex sea-level changes resulting from interrelated eustatic, glacio-isostatic, and hydro-isostatic forcings, and local climate evolution (Forbes and Syvitski, 1994; Forbes et al., 1995; Orford et al., 1996; Forbes, 2005). Detailed knowledge of the distribution and thickness of all sediments in such a system, and the history of local relative sea-level changes, permit reasonable estimates of the timing of sediment erosion and deposition in late Holocene barriers and estuaries and can place constraints on the duration of the local paraglacial period. Furthermore, such quantification can elucidate the role of various coastal processes in the development of these barrier systems as they evolve beyond their paraglacial setting. For example, an overwhelming majority of these studies on barrier-island formation have focused on barriers formed in coastal plain settings, specifically the southern and eastern margins of United States (e.g., see Smith et al., 2010) where sediment is generally abundant and tidal ranges relatively small. The resulting theories focus on wave action as the dominant mechanism driving the evolution of barrier systems; the effects of changes in tidal exchanges between backbarriers and the open ocean through time on barrier development is rarely investigated. However, Tye and Moslow (1993) report that inlet-fill sequences can account for as much as 30–50% of barrier lengths, even in wave-dominated settings. In recent decades, detailed GPR and shallow-seismic techniques have allowed for the identification of such tidal-inlet-fill sequences and determined that they often possess a range of sedimentologic characteristics and reflection geometries (Siringan and Anderson, 1993; FitzGerald et al., 2001; McBride et al., 2004; Rieu et al., 2005). These sequences are identified throughout much of the

111 world, but are largely related to historical and/or ephemeral inlets, and therefore are unrelated to
112 the likely role of tidal inlets in early barrier formation.

113 The goal of this study is to provide the first detailed sedimentologic and geophysical
114 examination of Plum Island, a mid-latitude paraglacial barrier system and the longest barrier
115 island in the Gulf of Maine. It relies upon geophysical, sedimentologic and geochronologic tools
116 for the reconstruction of the developmental history of the barrier and its associated backbarrier,
117 marsh and inlet systems in response to changes in sediment supply and the rate and direction sea-
118 level change. We present an updated stratigraphic framework and a refined, process-based
119 evolutionary model that focuses specific attention on the various glacial and non-glacial
120 sediment sources that have contributed to the development of the barrier. Furthermore, we seek
121 to present an updated geochronological framework for barrier development in northern
122 Massachusetts and highlight, for the first time, the vital early role played by inlet closure in
123 barrier-island formation.

124

125 **2. Study Area**

126 ***2.1. Physical Setting***

127 Plum Island is located in the Merrimack Embayment, a mixed-energy, tide-dominated, inlet-
128 influenced (FitzGerald and van Heteren, 1999) section of coast in northern Massachusetts
129 (western Gulf of Maine) extending north from Cape Ann into southern New Hampshire (Fig. 1).
130 This site provides an ideal location for the study of Holocene paraglacial barrier-island formation
131 due to its well-documented sea-level history (Section 2.2; Fig. 2) and diverse fluvial and glacial
132 sediment sources, including the Merrimack River, one of the largest estuaries in the Gulf of
133 Maine.

The Merrimack Embayment barrier system (Seabrook Beach, Salisbury Beach, Plum Island, Castle Neck, Coffins Beach, and their associated tidal inlets, estuaries and backbarrier sand flats, channels and marshes; Fig. 1) is the longest in the Gulf of Maine, spanning 34 km. Barriers in this chain are pinned to bedrock and/or glacial promontories. Tidal inlets commonly are situated in drowned river valleys and the barriers are backed primarily by marsh and tidal creeks that typically enlarge to small bays near the inlet openings (Smith and FitzGerald, 1994). Though several of these inlets have some freshwater influx from nearby streams (e.g. Parker and Essex Rivers; Table 1), flow in these rivers is dominated by tidal fluxes. The only estuary with significant freshwater discharge is the mouth of the Merrimack, a drainage system that has its headwaters in the White Mountains of New Hampshire and a catchment of approximately 13,000 km^2 along its 180 km course to the ocean. The Merrimack drains regions dominated by granitic plutons that have been eroded to produce quartzose, sandy glacial deposits. The lower part of the river flows through coarse, sandy ice-marginal deltas that formed along the retreating ice front at the glaciomarine sea-level highstand and in subsequent glacial lakes up valley (Stone et al., 2006). In its coastal reach, the Merrimack River flows over bedrock and enters a small bay at its mouth, landward of the barrier system. This bay contains extensive tidal sand flats, including flood-tidal sand at the northwest end of Plum Island and overlying proximal sections of jetties that were constructed in the early twentieth century. Seaward of the Merrimack River Inlet, the ebb-tidal delta extends in a southerly direction. Modern bedload sediment discharged through this inlet ranges in size from fine to coarse sand and granules (FitzGerald et al., 2002). Southerly- and ebb-oriented bedforms within this ebb delta complex indicate southerly migration. This corroborates sedimentologic evidence showing a southerly fining trend in grab samples collected across the ebb delta and a general trend of increasing textural and

mineralogical maturity to the south, away from the Merrimack River, reflecting winnowing and differential transportation of finer sand grains by wave action (FitzGerald et al., 1994). Together, this evidence demonstrates the dominance of southerly longshore currents and the continued contribution of sediment to the barrier system by the Merrimack River.

2.2. Sea-Level History

The late Quaternary sea-level history of the Gulf of Maine has been studied in detail by a number of authors (Kaye and Barghoorn, 1964; Belknap et al., 1987; Birch, 1990; Kelley et al., 1992; Barnhardt et al., 1995). In the Merrimack Embayment, Oldale et al. (1983, 1993) built on the earlier work of McIntire and Morgan (1964), and presented a post-glacial relative sea-level curve controlled by the depths and ages of a submerged marine lowstand delta of the Merrimack River, coastal features on Jeffreys Ledge (northeast of Cape Ann), and younger Holocene salt-marsh deposits (Fig. 2). Stone et al. (2004) modified the postglacial model of Kaye and Barghoorn (1964) by combining the detailed glacioeustatic sea-level curve of Fairbanks (1989) and a crustal uplift curve based on glacioisostatic parameters (Koteff et al., 1993; Stone and Ashley, 1995), which predicted a longer period of sea-level lowstand. Donnelly (2006) presented an updated, calibrated curve for northern Massachusetts for the past 4000 years based on radiocarbon dates from basal high-marsh peats.

Relative sea-level changes in this region have resulted from the combined forcings of global eustatic sea-level rise, and regional glacio- and hydro-isostatic adjustments. Following the last glacial maximum (28.0–23.7 ka; Stone and Borns, 1986) and retreat of the ice margin into the Gulf of Maine, sea level in Massachusetts rose rapidly over the isostatically depressed region in response to the global influx of glacial meltwater. The maximum synglacial marine limit in the

Merrimack embayment was reached at 17-16 ka (Stone and Borns, 1986; Ridge, 2004; Stone et al., 2004) at elevations of 31–33 m above mean sea level (m MSL, measured in North American Vertical Datum 1988 [NAVD88]) (Stone and Peper, 1982). Rapid isostatic rebound resulted in a marine lowstand at 13–14 ka (Table 2; Fig. 2) estimated at -41 m MSL (Hein et al., 2010). Following this lowstand, the Holocene sea-level rise progressed relatively rapidly and episodically for the first several thousand years (Oldale et al., 1993; Fig. 2), but by 4–5 ka, relative sea-level rise had slowed to near modern rates (0.6 ± 0.1 m/yr; Donnelly, 2006).

2.3. Previous Work

Several hypotheses have been suggested regarding the formation of the Merrimack Embayment barrier system. Based on comparison to the drowned drumlin field of the Boston Harbor Islands, Chute and Nichols (1941) proposed that the barriers in the Merrimack Embayment formed relatively recently, from the erosion and reworking of drumlin till deposits during the latest stages of the modern transgression. Based on a series of nearly 60 sediment cores and eight radiocarbon dates, McIntire and Morgan (1964) presented a six-stage model for the development of the Merrimack Embayment barrier system. This model was the first to place various sedimentological units in their chronologic context and treat the evolution of the barrier system with respect to a variable sea level. In their model, beach sediments were deposited directly on glaciomarine clay during post-glacial, rebound-induced sea-level fall. The shoreline transgressed subsequent to crustal uplift and maximum sea-level lowstand, reworking the older regressive strand deposits into beaches. In this model an initial barrier formed at 6.3 ka and migrated landward to its present location, which it reached within the last 3000 years. This

model supports sediment sources from the transgressing coastal zone and from the Merrimack River.

Initial geophysical investigations of the shallow shelf of the Merrimack Embayment (Oldale et al., 1983, Edwards, 1988) revealed the extent of the submerged Merrimack River lowstand delta located 6–7 km offshore and trending parallel to the present coast. The delta is 20 km long, 4–7 km wide, up to 20 m in thickness, contains ~1.3 billion m^3 of sediment and lies beneath 41–50 m of water (Oldale et al., 1983; Oldale et al., 1993). Seismic profiles show that a planar, gently seaward-dipping erosional surface truncates the upper parts of easterly-dipping delta foresets, indicating that the distal surface of the delta was deeply scoured during the early Holocene transgression of the region (Oldale et al., 1983; Barnhardt et al., 2009). FitzGerald et al. (1994) recognized the importance of the Merrimack paleodelta as a potential sediment source for the transgressing shoreline and suggested a four-stage developmental history for the barriers: sediments of the upper paleodelta were eroded during the early transgression, reworked shoreward as an expansive sand sheet, pinned to drumlins, shallow till and bedrock at 4–5 ka, and have since built vertically and prograded seaward.

3. Methods

Nearly 20 km of ground-penetrating radar (GPR) data were collected along shore-parallel and shore-normal transects (Fig. 3) using a Geophysical Survey Systems Inc (GSSI) SIR-2000 system with a 200 MHz antenna. This system produced reflection data to -3 to -7 m MSL, depending on the proximity to backbarrier marshes and the associated brackish ground-water table. Five km of GPR data to -13 to -16 m MSL were collected using a Mala Pro-Ex system with a 100 MHz antenna. All GPR data were post-processed (site-specific data filtering,

variable-velocity migration, gain control) using a combination of Radan (GSSI), RadExplorer (DECO-Geophysical Co. Ltd.), and GPR-Slice (Geophysical Archaeometry Laboratory) software packages. Time-depth conversions were completed using relative dielectric permittivities (Neal, 2004) for unsaturated (2.55–7.5; upper ~1-2 m; location dependent) and saturated (20–31.6; upper ~1-2 m; location dependent) sand and ground-truthed with sediment cores. Nearly 13 km of shore-parallel post-processed GPR data were analyzed for reflectionreflection characteristics and dip components. Some shore-normal profiles also were analyzed in the same manner. True dip attitudes of reflectionreflections were determined at profile intersection points. Descriptive terminology of radar reflectionreflection geometry is derived from van Heteren et al. (1998) and Neal (2004). Published post-processed chirp shallow seismic reflection profiles in the nearshore of Plum Island (Barnhardt et al., 2009) were used to map the distribution of nearshore cut and fill structures associated with major channel systems (Fig. 4).

A suite of 30 cores ground-truthed time-depth conversions and verified stratigraphic units inferred from the GPR-reflection profiles (Fig. 1). All cores were collected at sites between -2 and +1 m MSL, along the landward side of the barrier. Seven vibracores provided detailed stratigraphy in the top 4 m of the island sequence. A Geoprobe Model 54DT direct push machine was used to collect 12 cores that retained fine stratigraphy and sedimentary structures to a maximum of -15 m MSL. Deep samples were collected from 11 auger cores that penetrated to as much as -36 m MSL using a truck-mounted Mobile B-40 auger drill rig. Sediment samples from all cores were prepared and analyzed using combined wet/dry sieve techniques to determine particle-size characteristics (Folk and Ward, 1957); mineralogical classifications (via hand-picking) were completed for a series of randomized samples to confirm visual observations. For

248 samples with >10% mud, fine fractions (<0.5 mm) were separated by wet sieving and analyzed
249 using a Beckman Coulter LS 13 320 Laser Diffraction Particle Size Analyzer (LDPSA).
250 Ten mollusk, wood, and peat samples were selected from cores for accelerator mass
251 spectrometer radiocarbon analysis (Table 3). As no mollusk samples were found in articulated or
252 growth position, individual samples were selected for dating based on quality of preservation and
253 stratigraphic context.
254
255 **4. Results: Chronostratigraphic Framework and Geophysical Units**
256 Major lithologic boundaries were determined from sediment cores (Figs. 5, 6) and shallow
257 (200 MHz antenna; maximum depth penetration of -3 m MSL) and deep (100 MHz antenna;
258 maximum depth penetration of -16 m MSL) GPR reflection profiles (Figs. 7, 8, 9). Calibration of
259 published ages and results of new radiocarbon analyses are presented in Tables 2 and 3,
260 respectively. New calibrated dates from this study are plotted on a generalized Holocene sea-
261 level curve for northeastern Massachusetts (Fig. 10). Onshore sedimentologic and GPR facies are
262 divided into eight stratigraphic units:
263
264 ***4.1. Unit I***
265 This basal unit is not shown in the GPR profiles and is known only from correlation with the
266 lowest unit in offshore seismic stratigraphy (Barnhart et al., 2009; Hein et al., 2010), and with
267 exposed deposits of drumlin headlands and basal deposits on the mainland. The top of this unit
268 appears as a strong, continuous reflection with occasional parabolics in radargrams and seismic-
269 reflection profiles. These reflections continue into areas of bedrock outcrops or regions of thin
270 till deposits between basins filled with layered sediments. Deeper sections of this unit are
271 acoustically transparent. Unit I includes bedrock and overlying thin till (<3 m thick), and thick

till deposits in drumlins; it is exposed as two drumlins at the southern end of Plum Island where they contain an unsorted, non-stratified matrix of fine sand, silt, and clay containing scattered gravel clasts and a few large boulders.

4.2. Unit II

Unit II is laterally continuous across the study area (Figs. 5, 7). It contains very few horizontal, discontinuous internal reflections and is dominated by data noise. Due to its fine-grained composition, the upper boundary of this unit generally determined the depth limit of GPR penetration. This upper contact (-6 to -22 m MSL) mirrors underlying bedrock topography (right side, Fig. 5) and is marked by a strong, highly irregular reflection in GPR profiles (Fig. 7) that is evidence of intense erosion. In our deepest core (PID02), Unit II is ≥15 m thick (Figs. 5, 6a). Sediment cores reveal that Unit II is heterolithic, composed of interbedded very fine sand, silt, silty-clay, and fine clay, with, rare, isolated pebbles and cobbles. This unit is laminated and highly compacted and dewatered. The lower portion is nearly all silty-clay and clay and is massive to thinly laminated; the uppermost section (0.5–2 m) is non-uniform and typically composed of indistinctly laminated olive green (5Y 4/2; Munsell Color, 2000) to brown (10YR 2/2) oxidized clay with some lenses of laminated organic-rich clay.

4.3. Unit III

Unit III contains weak, horizontal to sub-horizontal (<2^{o} dip) discontinuous reflections in GPR profiles, with little discernable pattern (Figs. 7, 8, 9). Chaotic reflection are common, as are small-scale (<1 m, horizontally) truncations of individual clinoforms. Locally, reflectors pinch out laterally and are generally indistinct. Where the basal reflector of Unit III is visible in

radargrams, it is generally present at -7 to -11 m MSL. GPR profile and core data indicate that 6–10 m of Unit III sand unconformably overlies finer silts and clays of Unit II immediately above an erosional unconformity. Unit III is nearly homogeneous, massive, moderately well-sorted fine sand and silt dominated by quartz but locally containing >10% muscovite mica and traces of organic materials.

Detrital (reworked) organic material collected for radiocarbon analysis was obtained from the lowest beds of Unit III at the basal transgressive unconformity above Unit II (Table 3). The oldest, 8781 ± 171 BP, is from a disarticulated bivalve collected from within a 1-m thick bed of fine, shell-hash rich sand at -17.7 m MSL (core PID05). A second mollusk fragment from a layer of poorly-sorted fine to coarse sand, pebbles, and shell hash at -15 m MSL (core PID11) yielded a date of 6789 ± 138 BP. The third date, 8085 ± 87 BP, from a 25-cm thick, partially decomposed tree branch at -11.6 m MSL (core PID03) was found within a 1.5-m thick intertonguing transition between fine, mica-rich sand (Unit III) and laminated clay (Unit II).

4.4. Unit IV

Deep GPR profiles revealed the erosional boundary of a 40-m wide U-shaped depression cut through strata of Unit III to the top of Unit II, located at a depth of -9 to -11 m MSL (Fig. 7). This depression is part of a larger U-shaped feature, 8 m deep and 100 m wide at its maximum. This feature is bounded by the horizontal to sub-horizontal reflectors of Unit III to the north and south and Unit VI above it. A series of eight parallel GPR transects spaced 8–10 m apart revealed that this feature is a spatially-continuous east-west-trending (shore-normal) channel. At the base of Unit IV is a 5-cm thick layer of mixed coarse sand to large pebbles with interstitial fine sand (Fig. 6b, 7). This is the coarsest and most heterogeneous sediment discovered in the

barrier sequence. The basal gravel is overlain by a 25-cm sequence of small, subangular pebbles in a matrix of very-coarse sand and granules that fines upward to medium sand; this is in turn overlain by nearly 7 m of flat-bedded, medium to coarse sand (Fig. 6b). Unit IV is, on average, approximately 1 phi coarser than surrounding sediments of Unit III.

4.5. Unit V

GPR profiles (Fig. 8a) show a high-amplitude reflection at the base of Unit V. This forms a U-shaped channel about 4 m deep and 700 m wide that trends shore-normal across Plum Island southeast of the Parker River mouth. Unit V can be divided into two complexes: a 3.5-m thick northern section dominated by southerly dipping reflections (Unit V-a); and a (2–4 m) southern complex of variable thickness (Unit V-b; Fig. 8a). At its northern end, the basal reflection of Unit V-b dips nearly due south at approximately 8^{o}, strongly truncating the upper portion of Unit III. This reflection becomes horizontal at -6.5 m MSL where it correlates with a 5-cm-thick poorly-sorted medium- to very-coarse sand at -6.7 m MSL (Fig 8b). Highly-decayed organic matter was collected from within this unit for radiocarbon analysis.

Internal reflections of Unit V-b are very complex, marked by various dip directions and angles. At its northern end, internal reflections consist of a series of sub-parallel, southward-dipping, sigmoid-oblique reflections, sub-horizontal ($<2^{o}$ dip) at the top, $11–13^{o}$ in the middle 3 m, and flattening to horizontal at the bottom where they intersect with the strong basal reflection (Fig. 8b). These strata are composed of thinly laminated medium-coarse sand interbedded with coarse sand, medium sand, and local fine sand, organic laminae, and thin concentrations of heavy minerals. To the south, reflections in this series are deeper and appear to have undergone erosion of the upper 1 m as seen by the presence of multiple reflection truncations. This series pinches

out to the south, replaced by complex, horizontal to sub-horizontal and undulating reflections overlying the Unit V basal reflection. About 150 m farther south this horizontal series is interrupted by a second, 80-m wide, 2.5-m thick sequence of southerly dipping sigmoid-oblique reflections. True dips range from 1.5^{o} to 4^{o}. This second sequence also pinches out to the south, due in part to the shallowing basal section of the unit. The southernmost 100 m of Unit V-b is ≤2 m thick and composed of a wide, U-shaped reflection set, dipping at most 1–2^{o} (Fig. 8b).

4.6. Unit VI

Unit VI is generally <1 m thick and spatially discontinuous. It is composed of organic-rich very fine sand, silt, and clay with abundant root fragments of *Spartina patens* (saltmeadow cordgrass). Unit VI was not identified in GPR profiles due to lack of penetration owing both to a shallow saltwater table and the fine-grained nature of the sediment. Sediment core data from the southern 1/3 of Plum Island reveal that it is located between Units III and VII, at -4 to -5 m MSL. Two dates were obtained from Unit VI. The lower date, 3286 ± 79 BP, is from the base of basal peat that overlies the medium fine sand typical of Unit III. The upper sample, 2215 ± 112 BP, was collected from the top of this basal peat sequence. Both new dates plot on the calibrated regional sea-level curve (Fig. 10).

4.7. Unit VII

Unit VII varies between 3 and 8 m thick along the length of Plum Island. It is characterized by complex, inclined GPR reflections, displaying highly-variable dip directions and angles. The base of Unit VII displays 2 m of erosional relief, resting on sandy, flat-lying strata of Units III and V. Surface eolian dunes overlie Unit VII. Sediments of Unit VII are composed generally of

quartz-rich medium- to coarse-grained sand and fine granules with occasional centimeter- to decimeter-thick heavy mineral concentrations. Along the 13-km length of the island, this unit can be generally subdivided into five sectors based on distance in kilometers (KM) southward from the Merrimack River Inlet:

4.7.1. KM 0–1.5

This northern-most sector is dominated by a shallow salt water table and complex to chaotic reflection geometries. Penetration was generally less than 3 m, revealing only the upper, anthropogenically modified section of Units VII and VIII.

4.7.2. KM 1.5–5.0

GPR penetration in this sector was generally 4–6 m. It is dominated by continuous horizontal, sub-horizontal, and subtly undulating (<1^{o} dip) reflection. Internal 10–20-m wide sections of 0.5–1.5-m thick packets of southward-dipping reflections (5–7^{o} dip) buried 3–4 m below the surface are common. At this same depth, several 30–35 m wide sections of northward-dipping packets also are present. These have shallower (3–4^{o}) dips and are <1.5 m thick. Both types of reflection packets tend to be sigmoid in form, flattening to horizontal with depth.

4.7.3. KM 5.0–9.0

This sector of Unit VII is dominated by a series of reflection packets that vary greatly in thickness (2–6 m) and dip angle (1–7^{o}) (Figs. 8, 9). Individual reflections in several sets can be traced >100 m, dipping at 1–2^{o} in the upper 4 m of the profiles. Shore-normal transects reveal that true dips are 2.5 –4^{o} to the south-southeast. These reflections are dominantly sigmoid-

oblique in shape, becoming sub-horizontal (<1^{o} dip) near the base. Individual reflections locally truncate one another and reflection sets commonly are underlain by stronger reflections, indicating alternating erosion and deposition. Also common are toplapping and offlapping sigmoid-oblique northwestward-dipping reflection sets (3–4^{o} dips) that downlap onto underlying southerly dipping reflection(Fig. 8a). Typically these are no more than 10–30 m wide and <1 m thick but can reach up to 200 m wide and nearly 3 m thick. These downlap onto the sub-horizontal reflections of Unit III and are overlain by thinner (1–2 m) packages of southerly dipping reflections (Fig. 9). At the southern end of this sector, a 160-m wide, 3-m thick U-shaped channel feature is visible. Internal reflections dip 5–7^{o} towards the center of this feature, downlapping onto a strong basal reflection. This feature has some morphological similarities to Unit V, but it is significantly smaller and is fully located within Unit VII. An auger core collected through the northern edge of this feature did not contain any coarser sediment corresponding with the basal reflection of this feature.

4.7.4. KM 9.0–11

Along this sector of Plum Island, available paths for data collection were proximal to the adjacent marsh platform. Shallow salt water resulted in penetration of ≤4 m and commonly ≤1 m. Where visible, Unit VII shows a similar form to that described for KM 6.0–9.0.

4.7.5. KM 11–13

Reflections in Unit VII are laterally discontinuous and chaotic in this sector of Plum Island. Small, 10–20 m long packets of shallow (2–3^{o}) southerly- and northerly-dipping reflections are rare.

4.8. Unit VIII:

Anthropogenic excavation and compaction for road construction commonly dominate the upper 1 m of all GPR profiles. Into this ubiquitous upper-most unit are lumped all modern facies: beach, dunes, modern soil in fields, and anthropogenic fill along roads. Along the landward side of the barrier, this unit is thin (<1 m) and has undergone anthropogenic modification and flattening for road construction.

5. Discussion

5.1. Barrier Stratigraphic Framework:

Unit I includes bedrock and till deposits of the last two glaciations. It is overlain by the draping deposits of Unit II, known in the Merrimack Embayment area as the Presumpscot Formation. This is a glaciomarine clay unit deposited in coastal Maine during deglaciation and the post-glacial highstand of sea level (Bloom, 1960), equivalent to the Boston Blue Clay of Kaye (1961) in the Massachusetts Bay area. Although no new cores penetrated to underlying till or bedrock, this unit has been shown to range in thickness from a thin drape (<1 m) to >30 m (McIntire and Morgan, 1964; Rhodes, 1973; Stone et al., 2006, Barnhardt et al., 2009) throughout the Merrimack Embayment; under Plum Island, it is ≥15 m thick (Figs. 5, 6a). On land (Sammel, 1963) and in our cores the Presumpscot Formation coarsens upward, reflecting its deep-water origin followed by increasing silt and sand components, perhaps indicative of increased glacial meltwater inputs during deglaciation of the coastal areas to the north, or increased input from the Merrimack River drainage. Solitary pebble and cobble dropstones reveal the presence of glacial, coastal, or river ice during sedimentation of most of the unit. The

presence of an oxidized uppermost portion of the glaciomarine unit and the overlying organic-rich mud evince a prolonged interval (perhaps 10^3 yrs) of subaerial exposure during the post-glacial marine regression and the late Pleistocene lowstand.

Overlying the glaciomarine clay, McIntire and Morgan (1964) identified a <1-m thick layer of freshwater peat, which has an age of ~7.2 ka (Table 2). They interpreted this as the leading edge of the Holocene transgression and incorporated it at -14.6 m MSL in their sea-level curve. This unit was not discovered in any of the 12 cores presented in this study that penetrated to the glaciomarine clay (Unit II). Rather, glaciomarine clay is unconformably overlain by Unit III, interpreted as consisting of transgressive estuarine and backbarrier facies. The youngest date (*PID11-S28:* 6789 ± 138 BP) was collected at -15 m MSL and is in best agreement with the more reliable basal freshwater peat date of 7.2 ka at -13.3 m MSL (McIntire and Morgan, 1964). Older dates (*PID03-S19:* 8085 ± 87 BP; *PID05-S15:* 8781 ± 171 BP) likely reflect reworking of older materials. Specifically, the 8.1 ka date derived from wood fragments at -11.6 m MSL likely originated from a transported tree fragment. Overall, dates from these samples present a wide range of possible ages for the Holocene flooding of this area. The samples were collected along the highly irregular and erosive unconformity between Units II and III and only the oldest of these dates plots close to the early Holocene portion of the calibrated sea-level curve for this region (Fig. 10). The shell fragments indicate coastal erosion to depths of 1–5 m for 2000–1000 years before their deposition in barrier beds beneath the stable backbarrier deposits of Unit II. Therefore, no indicative meaning of paleo-sea level is assigned to these dates. They can, however, be used as a guide to the geochronologic framework of deposition, indicating that the hiatus between Units II and III occurred between 6.8 and 8.8 ka and, based on the regional sea-level curve, was related to the flooding of the region occupied by modern Plum Island during the

Holocene marine transgression. Several additional radiocarbon ages from samples obtained within Unit III cluster between 3.5 and 6.7 ka, reflecting a >3000-year period of deposition for this 11-m thick section of nearly homogeneous medium-fine sand.

The late Holocene barrier-spit facies (Unit VII) overlies the backbarrier facies and contains sediment that strongly resembles the sand and fine gravel of the modern beach environment. This unit is interpreted to be chiefly the product of a southerly-migrating and seaward-prograding spit sequence. However, the dominant processes that formed Plum Island varied along shore, allowing sub-division into four sectors:

A) River- and Inlet-Modified (KM 0–1.5): This northernmost sector of Plum Island, tied closely to the adjacent Merrimack River and its inlet and ebb-tidal delta, shows evidence of recent modification. GPR and coring studies (Costas and FitzGerald, 2011) on Salisbury Beach, north of the Merrimack River, demonstrate the influence of fluvial and inlet modification in this region. Likewise, the formation of “The Basin” and the entire eastern fork of northern Plum Island have been attributed to the welding of onshore-migrating bars following the breach of the modern Merrimack Inlet (FitzGerald et al., 1994).

B) Aggradation/Progradation-Dominated (KM 1.5–5): The prevalence of seaward-dipping clinoforms identified in shore-normal GPR profiles throughout this sector in Unit VII demonstrates that it was formed predominantly by progradation and aggradation. Small packets of northward, southward, and westward dipping reflections are interpreted as the onshore migration and welding of small nearshore sand bars, driven by dominant southerly-longshore transport and, to the north, wave refraction around the adjacent southward extension of the Merrimack ebb-tidal delta. Southerly-dipping clinoforms become more common in shore-parallel

profiles in the southern 0.5 km (KM 4.5 – 5.0) of this sector. This marks a zone of transition to the spit-dominated regime to the south.

C) Spit-Dominated (KM 6–11): Unit VII along much of this sector is up to 6 m thick and is dominated by extensive sigmoid-oblique southeasterly-dipping reflections interpreted as welded ridge and channel margin platform facies (Hayes and Kana, 1976) of a southerly-prograding spit. Northwestward-dipping sections are interpreted as small bars associated with the recurved portion of the spit. These bars overlie the uppermost backbarrier facies (Unit III). They were intertidal to supratidal and served as the platform onto which the spit built.

D) Spit-Dominated, Inlet- and Drumlin-Influenced (KM 11–13): Unit VII in this southern-most part of the island is also spit dominated but retains ample evidence of influence by nearby glacial deposits, identified by Sammel (1963) as drumlin till. Modern spit progradation continues south of a 0.2-km^2 subaerial drumlin outcrop, where a 500-m wide spit platform extends into the modern Parker River Inlet. A 1.2-km long, subaerial recurved spit is evidence of continued influence of this inlet.

5.2. The Lowstand Parker River (Unit IV)

Shallow seismic-reflection data from the shallow shelf offshore of central Plum Island revealed a series of channel cut and fill structures eroded 5–10 m into the uppermost section of the underlying glaciomarine clay (Barnhardt et al., 2009, Fig. 4.11). These features are 100–200 m wide and are found as far as 4.2 km offshore, which was the seaward limit of high-resolution seismic data for that study. The pattern of these cut and fill structures bifurcates in a landward direction (Fig. 4). The northern set appears to track landward toward the mouth of the Parker River, which presently drains into Plum Island Sound. These features also are aligned with Unit

IV, which fills an elongate U-shaped channel eroded into the glaciomarine clay. The basal section of Unit IV is interpreted as a coarse lag deposit, unconformably eroded into the highstand glaciomarine Unit II (Figs. 6b, 7). Together, these features are inferred to be the preserved remnants of the extension of the paleo-Parker River onto the shallow shelf during a lower stand of sea level, prior to the final Holocene transgression and the formation of Plum Island.

The southwestern-tracking set of cut-and-fill features is similarly aligned with the modern mouth of the Rowley River (Fig. 4). However, a shallow saltwater table in this area reduced penetration of GPR to the upper 4 m of the barrier sequence, prohibiting onshore imaging of these channel features. An auger-drill core into the glaciomarine clay in this area revealed that the erosional contact is located at -15 m MSL. Here, the upper portion of the clay shows no evidence of subaerial exposure; rather the contact is sharp and likely erosional. However, the basal channel lag deposits seen in Unit IV are absent here, replaced by a coarse sand/shell hash layer. A mollusk sample from this unit was dated to 6.8 ka, which plots below the calibrated sea level curve (Fig. 10), and provides further evidence that this contact was indeed erosional. Therefore, while the extent of a secondary fluvial channel under Plum Island cannot be verified, the nature of the contact between the glaciomarine clay and overlying backbarrier facies suggests that erosional processes were active and may well have been related to a lowstand offshore extension of the Rowley River.

5.3. Paleo-Inlet Sequence (Unit V)

The repetitive southward-dipping GPR reflections of the barrier spit facies are interrupted by structures of Unit V approximately 100 m south of the buried channel of the paleo-Parker River. Here, Unit V is composed of a complex sequence of conformable, accretionary sets of southerly-dipping reflections punctuated by sharp truncation surfaces, cut–and-fill features and

smaller packets of northerly-dipping reflections (Fig. 8). Many of the features of this sequence in Unit V are characteristic of tidal inlet deposits within barrier lithosomes (Moslow and Herron, 1978; Tye, 1984; Tye and Moslow, 1993; FitzGerald et al., 2012). This sequence is interpreted as the remnants of a paleo-inlet (the "paleo-Parker Inlet") that once existed beneath what is now central Plum Island (Fig. 11b-d). Interbedded, fine-, medium- and coarse-sand units are interpreted as marking high energy depositional events associated with spit accretion and migration of the inlet southward. Northward-dipping clinoform sets are interpreted as the onshore migration of bars and their eventual welding to the beach associated with ebb-delta breaching events. Breaching resulted in a displacement of the inlet to the north, truncating the earlier inlet and spit reflections (Unit V-a: Inlet Complex I, Fig. 8) and eroding the underlying backbarrier facies (Fig. 8b). Further infilling of the inlet channel (Unit V-b: Inlet Complex II, Fig. 8) increased its propensity to migrate (e.g. FitzGerald et al., 2001), until it eventually shoaled completely and closed. A series of high-frequency, steeply-southeasterly-dipping reflections capture the rapid progradation of the spit system (Unit VII) across the closed inlet (Fig. 8a).

In GPR profiles, the top of the paleo-inlet sequence is denoted by the upper break in slope in the sigmoidal inlet-fill reflections at -3.5 m MSL, which also serves as an approximate reference for mean low water at the time the inlet was active. This suggests that MSL at that time was approximately 2.2 m below the modern level. Radiocarbon analysis of mixed organics collected within a coarse sand/granule bed at the base of the inlet sequence, -6.7 m below modern MSL, produced a date of 3597 ± 47 BP. The calibrated sea level curve is well constrained in its upper section (Fig. 10) and thus indicates that mean sea level at this time was approximately 2.6 m

547 below the modern level, similar to that determined from analysis of inlet-fill reflections.
548 Together, these data confirm that the paleo-Parker Inlet was active around 3.4–3.6 ka.
549
550 ***5.4. Evolutionary Model for Plum Island and Associated Barrier System***
551 *5.4.1. Sediment Sources*
552 Previous evolutionary models (see sect 2.3) proposed the reworking of drumlin till deposits
553 (Chute and Nichols, 1941) or the onshore reworking of regressive and lowstand fluvial and
554 shoreline sediments during the Holocene transgression (McIntire and Morgan, 1964; FitzGerald
555 et al., 1994) as sources of sediment for the development of the Merrimack Embayment barrier
556 system. However, each of these models provides an incomplete picture. For example, although
557 the modern coastal zone contains scattered drumlins (Fig. 1) and nearshore boulder-lag deposits
558 from eroded drumlins, these features are located only at the southern end of Plum Island. They
559 have an estimated combined volume of only ~4 x 10^6 m^3, a value dwarfed by even a rough
560 estimate of the sediment comprising the Plum Island barrier lithosome based on barrier thickness
561 and aerial dimensions (~75 x 10^6 m^3). Furthermore, sediment contributed by these features is
562 heterogeneous in texture and mineralogy, characteristics that contrast with the mature sand that
563 makes up the modern barriers.
564 Moreover, McIntire and Morgan (1964) and FitzGerald et al. (1994) recognized the
565 importance of shelf sources to the development of the Merrimack Embayment barrier system, but
566 largely dismissed direct fluvial contributions. Dredging operations from the Merrimack River
567 Inlet (E. O'Donnell, U.S. Army Corps of Engineers, pers. com., 2010) during a 62-year period
568 removed 2.6 x 10^6 m^3 of sand and gravel (average annual coarse-sediment deposition rate: 4.16 x
569 10^4 m^3/yr since the mid-1900s). This rate is likely a low estimate compared to periods in the

570 early Holocene, when the river was eroding proglacial deltas and sandy lake-bottom deposits,
571 exposed in the regions of glacial Lakes Merrimack and Hooksett (Koteff, 1970) and local lakes
572 in the lower Merrimack valley (Stone et al., 2006). Since that time, slope, terrace, and floodplain
573 deposits, and the river channel, have been stabilized by bedrock knick points, vegetation cover
574 and engineering structures. Additional anthropogenic modifications, such as the construction of
575 dams in the upstream reaches of the river, have further reduced sediment input to the coast.
576 However, even at modern rates of delivery of fluvial sand and gravel (4.16×10^4 m^3/yr), <2000
577 years are required for the deposition of the volume of sediment composing the Plum Island spit
578 system (Unit VII; ~75×10^6 m^3). Even if sediment loss to the shallow shelf, tidal deltas, and
579 other barriers along the Merrimack Embayment barrier chain are accounted, fluvial sediment
580 from the Merrimack River was likely the dominant source of sediment for the formation of Plum
581 Island during the past 4000 years. Additional sediment was derived from deep erosion of the
582 Merrimack River lowstand delta and regressive braid plain delta with minor contributions from
583 the erosion and reworking of drumlin till deposits and small coastal rivers that currently drain
584 into Plum Island Sound (Table 1).
585
586 *5.4.2. Early Developmental History*
587 After final deglaciation in the Merrimack Embayment region (16–15 ka) a river-dominated
588 shoreline developed from continued meltwater flow from the Merrimack drainage basin,
589 coincident with rapid crustal rebound and sea level fall. The multiple river mouths and channels
590 followed the regressing shoreline, modified locally by bedrock and drumlin headlands. Coastal
591 and fluvial processes modified and redistributed fluvial sediment across the open embayment
592 that developed on the emergent surface plain of the Presumpscot Formation. This resulted in the

593 deposition of an 8–10-km-wide (perpendicular to shore), 16 km-long, and 4–15-m-thick
594 (Barnhardt et al., 2009) seaward-prograding, wave-smoothed offlap regressive braid plain delta.
595 This unit pinches out adjacent to the modern shoreline, due either to non-deposition during rapid
596 late Pleistocene rebound-induced regression, or due to erosion during the later stages of the
597 modern transgression (Barnhardt et al., 2009).

598 Approximately 2 km offshore of modern Plum Island, drainage from the Paleo-Parker River
599 merged with a second tributary (the Paleo-Rowley River?), and likely contributed sediment to
600 the developing braid plain delta and eventually the lowstand Merrimack delta. The final
601 disposition of sediment covering this deposit during the regression was forced by coastal, river,
602 and slope processes in a periglacial coastal environment at 16–14 ka, before the spread of
603 vegetation (Stone et al., 2004).

604 During the regional glacioisostatic marine lowstand of approximately -41 m at 13–14 ka the
605 Merrimack River and to a lesser extent the Parker, Rowley and Ipswich Rivers continued to
606 supply sediment to the proximal braid plain delta and distal lowstand delta. Inner shelf
607 submerged channel cut-and-fill features were preserved in coarse channel lag and fill deposits,
608 such as those found offshore of the extension of the Parker River are an indication of the channel
609 system responsible for transporting sediment to the lowstand delta.

610 Shoreline migration during the Holocene transgression eventually flooded the lower reaches
611 of the lowstand Parker River channel and initiated upstream infilling. The shoreline reached the
612 area beneath Plum Island at 7–8 ka, and was accompanied by formation of a freshwater
613 (McIntire and Morgan, 1964) backbarrier marsh. As the transgression proceeded and the
614 shoreline migrated landward, the mouth of the Parker River, located within modern central Plum

615 Island at this time, was tidal. Active tidal flow resulted in the deposition of the thick medium to
616 coarse sand sequence within this paleo-channel.
617
618 *5.4.3. Barrier Formation: Landward Migration and Backbarrier Deposition*
619 Continuing, but slowed, marine transgression drove sediments from coastal and river
620 sources farther onshore and fed the incipient Merrimack Embayment barrier system (Fig. 11a).
621 Deposition of the 6–10 m-thick sequence of fine sand composing the backbarrier and estuarine
622 facies presently underlying Plum Island requires lagoon protected semi-open-water lagoonal
623 environment. This confirms that when these fine sands were deposited, a proto-barrier existed
624 offshore of modern Plum Island, likely consisting of several discrete islands (Fig. 11a).
625 The backbarrier sediment generally was derived from offshore sources and moved onshore
626 by wave and tidal processes coincident with the landward migration of the barrier system. At this
627 time, fine sand was transported by tidal currents to the backbarrier through inlets. Minor
628 sediment was likely derived from upland deposits (i.e. bluff erosion, small streams with local
629 drainages, etc). McCormick (1969) collected more than 50 sediment cores in this unit and
630 determined that two facies are present: a finer unit dominated by fine sand and mud located
631 adjacent to mainland upland areas; and a coarser unit composed of fine to medium-coarse sand
632 located along the landward side of the barrier and proximal to tidal channels. These deposits
633 reflect both overwash processes and tidal reworking that contributed to the deposition of this
634 unit.
635
636 *5.4.4. Inlet Development, Evolution and Closure*

637 Although continued sea-level rise during the late Holocene forced the landward migration of
638 proto-barriers, their lateral growth was due to spit elongation produced by the dominant northeast
639 storm slimate and southerly longshore sand transport. In central Plum Island, the Parker River
640 partially infilled, but maintained a shallow tidally-influenced channel. By approximately 3.6 ka,
641 this channel had migrated southward and evolved into a moderate-sized tidal inlet (Fig. 11b).
642 This phenomenon of an inlet occupying former, highly erodible lower stand river channels is
643 well documented (Morton and Donaldson, 1973; Halsey, 1978; Tye, 1984; Imperato et al., 1988;
644 Siringan and Anderson, 1993; Levin, 1995; Rodriguez et al., 2000; and Kulp et al. 2006, 2007).
645 The paleo-Parker Inlet underwent a complex evolutionary development as recorded in the
646 sedimentary record beneath Plum Island; this included thalweg migration, ebb-delta breaching,
647 onshore bar migration, channel shoaling, and eventual closure (Fig. 11c-e). As mapped using
648 GPR and sediment-core data, remnants of this inlet cover an area of 2800 m^2 within the Plum
649 Island lithosome (Fig. 8a). However, this is a maximum estimate, as migration of the inlet would
650 leave a sedimentological signature across a wider area than the inlet ever occupied at a single
651 time, leading to ambiguity in interpreting the GPR signature of the inlet. Nonetheless, the cross
652 sectional area of the paleo-Parker inlet fill sequence can be used to provide insights into the
653 filling of the Plum Island backbarrier. Jarrett (1976) used an empirical approach to relate tidal
654 prism, defined as the volume of water entering or leaving a tidal inlet during a half tidal cycle, to
655 inlet cross-sectional areas. For example, for United States Atlantic coast inlets with one or no
656 jetties, Jarrett (1976) determined the following relationship:
657 $$A = 5.37 \times 10^{-6} TP^{1.07} \quad (1)$$
658 where A is the minimum cross sectional area of the inlet below mean sea level (in ft^2) below
659 MSL and TP is the spring or diurnal tidal prism transmitted through that inlet (in ft^3). Applying

660 this equation to the paleo-Parker Inlet at its maximum extent shows that it could have exchanged
661 as much as 36 x 10^6 m^3 of water between the open ocean and the backbarrier. This estimate is
662 only 10% greater than the tidal prism flowing through the modern Parker Inlet at the southern
663 end of Plum Island (32 x 10^6 m^3; Vallino and Hopkinson, 1998) and approximately 30% more
664 than nearby Merrimack River and Essex Inlets, whose values were determined using Jarrett's
665 method and published cross-sectional areas (Table 4). This indicates that the paleo-Parker Inlet
666 was of the same order of size as modern inlets in this system.

667 Other inlets must have existed simultaneously with the paleo-Parker Inlet. The large
668 freshwater discharge from the Merrimack River likely maintained an inlet at the northern end of
669 Plum Island throughout its development. Shallow bedrock and till identified in a series of cores
670 (McIntire and Morgan, 1964; McCormick, 1969) adjacent to Little Pine Island Creek, south of
671 the Merrimack River estuary (Fig. 1), provided a natural drainage divide, restricting the mouth of
672 the Merrimack River to an area near its modern course. Even at present, though Plum Island is
673 fully separated from the mainland, there is only limited exchange between Plum Island Sound
674 and the Merrimack River estuaries (Zhao et al., 2010).

675 Likewise, Parker River Inlet at the southern end of Plum Island has also been active
676 throughout the development of the island. This inlet is proximal to the Ipswich River, providing
677 an outlet for freshwater discharge and the southern Plum Island Sound tidal prism throughout
678 late Holocene time. This inlet is entrenched between two drumlins (Fig. 1), which has restricted
679 flows and caused scour to underlying till (FitzGerald et al., 2002). Barnhardt et al. (2009)
680 identified a channelized estuarine unit offshore of the southern end of Plum Island. This feature
681 is aligned with the modern inlet and is interpreted as an extension of the Ipswich River / Parker
682 River Inlet channel onto the shallow shelf during a lower stand of sea level, implying long-term

683 stability of an inlet at the southern end of Plum Island. Together, this indicates that there were at
684 least three active inlets along Plum Island around 3–4 ka, rather than just the two that exist today.
685
686 *5.4.5. Late-Stage Evolution: Marsh Development, Spit Elongation, and Barrier Progradation*
687 Late stage evolution of Plum Island was driven by spit elongation and barrier progradation.
688 The spit system overtopped the paleo-Parker Inlet (Fig. 11e) and extended to the south. Cores
689 collected along the landward side of Plum Island revealed the presence of a laterally
690 discontinuous, 1–1.5 m thick peat (Unit VI) between Units III and VII. A radiocarbon date from
691 the basal section of this peat (-2.6 m MSL) reveals that marsh growth initiated in this location at
692 3.3 ka. This date is in agreement with other published records of marsh growth initiation in New
693 England (Redfield, 1972; McIntire and Morgan, 1964; Kelley, 1995). A date from the uppermost
694 section of this peat indicates that here the barrier spit migrated on top of the marsh platform at
695 approximately 2.3 ka. This indicates that the southernmost 5 km of Plum Island formed since
696 that time, eventually topping intertidal shoals and anchoring to the drumlin at the southern end of
697 the island.
698 GPR reflections are horizontal to sub-horizontal along shore and shallowly seaward-dipping
699 cross-shore in the uppermost 1 m of the subsurface barrier lithosome along much of Plum Island.
700 This feature demonstrates the role of aggradation and progradation in the most recent latest
701 stages of barrier formation, allowing the barrier to maintain and expand its subaerial profile with
702 continued sea-level rise.
703
704 **6. Implications and Conclusions**
705 ***6.1. Sediment Sources and Coastal Processes: The "Paraglacial" Setting of Plum Island***

706 The model presented here greatly refines previous paradigms for the evolution of Plum
707 Island and the Merrimack Embayment barrier system and includes a variety of likely sediment
708 sources (direct glacial and fluvial sources and reworked shallow shelf material) and processes
709 (aggradation, progradation, spit elongation, inlet closure). Shallow, irregular bedrock relief, in
710 conjunction with glacial (till, Unit I), glacio-fluvial, and glaciomarine (glaciomarine clay, Unit
711 II) sediments, form the underpinnings of Plum Island and the associated barrier system
712 (backbarrier, inlets, etc.): till (Unit I) and glaciomarine clay (Unit II). The Merrimack River
713 delivered glaciogenic sediments to the coast where they then were deposited in a regressive braid
714 plain delta, lowstand marine delta, and a network of fluvial channels. During the Holocene
715 transgression these sediments were partially excavated and reworked, and combined with 1)
716 sediment released from eroding drumlins, and 2) continuing fluvial inputs, to form the proto-
717 barrier system in its early migrational and accretionary phases. The river channels and barrier
718 systems stabilized near their modern locations at about 2.5–3.5 ka. This marked the end of the
719 interval of barrier growth and stabilization as part of the paraglacial erosional/depositional
720 setting.

721 During the mid- to late-Holcoene, the Plum Island barrier system evolved solely in response
722 to spit progradation in a regime of slow sea-level rise: this accounted for more than 60% of the
723 island's length. Nearly 90% of its width is from seaward progradation, with only a minor
724 contribution from overwash and landward migration. The activity of the paleo-Parker Inlet is
725 associated with a change in the rate of sea-level rise in northern Massachusetts (Fig. 10),
726 implying that the transition from a migratory and accretionary system to one dominated by spit
727 elongation occurred quickly, and possibly simultaneously with the slowing of sea-level rise. The
728 continued extension and progradation of the barrier system required an increasing sand supply

729 (Dillon, 1971), which was provided, in this case, by the proximal Merrimack River. Plum Island,
730 now largely reliant on non-glacial sediment sources and responding to forcings in a manner
731 indistinguishable from a barrier in a non-glaciated setting, should be viewed as being beyond its
732 paraglacial period. Therefore, with a few localized exceptions (e.g. coastal drumlins presently
733 undergoing erosion), the Merrimack Embayment barrier system is in a "post-paraglacial" state.
734
735 ***6.2. Inlet-Fill Sequences in the Sedimentary Record: Implications***
736 Many studies have shown that inlet-fill sequences are a dominant feature in barrier
737 lithosomes (Moslow and Heron 1978; Moslow and Tye 1985; Tye and Moslow 1993; FitzGerald
738 et al., 2001). The preserved size, geometry, and facies of inlet-fill sequences depend on the
739 dimensions of the paleo-inlet (controlled by bay tidal prism), the migrational behavior of the
740 inlet (controlled largely by the dominant wave and longshore current regimes), and the factors
741 controlling the closure of the inlet (FitzGerald et al., 2012). In turn, each of these factors is
742 intimately related to the forces driving barrier evolution.
743 The paleo-Parker Inlet had a maximum cross-sectional area similar in size to the two
744 modern estuarine-mouth inlets that border Plum Island. When all three were active, they were
745 each maintained by the exchange of tidal waters between the backbarrier and coastal ocean. To a
746 first-order approximation, and absent of any landward barrier migration or additional sediment
747 supply, the gradual rise in sea level during the past 3600 years in northeast Massachusetts (Fig.
748 10) would have tended to increase tidal prisms, as additional upland areas became flooded. This
749 would cause a deepening and/or widening of local tidal inlets transmitting that prism (e.g.,
750 FitzGerald et al., 2006). By contrast, the presence of an inlet-fill sequence in central Plum Island
751 implies that the tidal prism in this system was once larger than at present. Backbarrier infilling

752 would have decreased the tidal prism passing through the paleo-Parker Inlet, resulting in
753 shoaling, a decrease in the inlet cross-sectional area, and eventual closure of the inlet. Such a
754 scenario has been demonstrated in other locations over more recent, shorter time periods. For
755 example, a 65% reduction in tidal discharges through Mason Inlet (North Carolina) in < 25 years
756 resulted in near closure of that inlet (Cleary and FitzGerald, 2003). Similarly, anthropogenic
757 changes at the Zoutkamperlaag Inlet system (Wadden Sea) resulted in a rapid (< 1 year)
758 reduction of the tidal prism by more than one-third, leading to rapid accretion and near closure of
759 the main inlet channel (Oost, 1995). Other studies have documented the shoaling and closure of
760 inlets through an incorporation of their tidal flows by adjacent inlet systems (Moslow and Tye,
761 1985; FitzGerald et al, 2001; Vila-Concejo et al, 2003). Finally, case studies along the west coast
762 of Florida (Davis and Bernard, 2003) and in the East Friesian Islands of Germany (FitzGerald et
763 al., 1984) have demonstrated the ability of anthropogenic modifications of backbarrier regions to
764 cause complete closure of one or more tidal inlets, thereby elongating and enlarging fronting
765 barrier systems.

766 The updated model presented here of sediment sources and coastal processes responsible for
767 the formation of Plum Island presented here represents the first time that the role of tidal inlets in
768 the formation and evolution of barriers along mixed-energy shorelines has been demonstrated.
769 Indeed, closure of the paleo-Parker Inlet allowed for the final aggradational and progradational
770 stages of barrier formation. Thus the discovery of the paleo-Parker Inlet within the Plum Island
771 barrier system is an example of the importance of inlet processes in the development of barrier
772 islands and provides the foundation for further investigation of the role of backbarrier infilling,
773 tidal prism reduction, and inlet closure in barrier-island evolution.
774

7. Acknowledgements

The authors would like to thank Drs. Robert E. Weems and Helaine W. Markewich of the U. S. Geological Survey (USGS) and two anonymous reviewers for their detailed revisions of earlier versions of this manuscript. Our deep appreciation also goes to Graham Taylor and the staff of the Parker River National Wildlife Refuge for their accommodation and assistance throughout the course of several years of field work. This study was funded by the Minerals Management Service (now the "Bureau of Ocean Energy Manegement, Regulation and Enforcement"), the USGS Eastern Geology and Paleoclimate Science Center, the USGS National Cooperative Geologic Mapping Program (State Map), a Geological Society of America (GSA) Student Research Grant, the American Association of Petroleum Geologists (AAPG) Grants-in-Aid program, and the Boston University Undergraduate Research Opportunities Program (UROP). Additionally, E. Carruthers was funded in part by the Clare Booth Luce Summer Research Fellowship and C. Hein was funded by the National Science Foundation (NSF) Graduate Research Fellowship.

The authors would like to acknowledge Mary Ellison, Nicholas Cohn, and Meaghan Gorman for their extensive assistance in the field and in the lab; Dr. Britt Argow for her assistance and use of the Wellesley College sedimetology lab and LDPSA. Brittany Schwartz, Susana Costas, Gene Cobbs, Jr. (USGS), Jeff Grey (USGS), Rachel Scudder, Carol Wilson, Christine Harrington, Thelma Scolaro, Nick Howes, Brandy Rinck, and Stephanie Simms also are acknowledged for their contributions in the field and lab.

8. References Cited

797 Ballantyne, C.K., 2002. Paraglacial geomorphology. Quaternary Science Reviews 21, 1935-
798 2017.
799 Barnhardt, W., Andrews, B., Ackerman, S., Baldwin, W., Hein, C., 2009. High Resolution
800 Geologic Mapping of the Inner Continental Shelf: Cape Ann to Salisbury Beach
801 Massachusetts: U.S. Geological Survey Open-File *Report OFR-07-1373*, 50 p.
802 Barnhardt, W.A., Gehrels, W.R., Belknap, D.F., Kelley, J.T., 1995. Late Quaternary relative sea-
803 level change in the Western Gulf of Maine: Evidence for a migrating glacial forebulge.
804 Geology 23, 317-320.
805 Belknap, D.F., Kelley, J.T., and Shipp, R.C., 1987. Quaternary stratigraphy of representative
806 marine estuaries: Initial examination by high resolution seismic reflection profiling, in:
807 FitzGerald, D.M., Rosen, P.S. (Eds.), Glaciated Coasts. Academic Press, San Diego, pp. 143-
808 176.
809 Birch, G.F., 1990. Phosphorite deposits on the South African continental margin and coastal
810 terrace, in Burnett, W.C., Riggs, S.R. (Eds.), Phosphate deposits of the world, Volume 3:
811 Genesis of Neogene to recent phosphorites. Cambridge University Press, Cambridge, pp.
812 153-166.
813 Bloom, A.L., 1960. Late Pleistocene changes of sea level in southwestern Maine. Maine
814 Geological Survey, Augusta.
815 Chute, N. E., Nichols, R. L., 1941. The geology of the coast of northeastern Massachusetts:
816 Mass. Dept. Public Works-U. S. Geological Survey Cooperative Geology Project Bull. 7, 48
817 p.

818 Cleary, W.J., FitzGerald, D.M., 2003. Tidal inlet response to natural sedimentation processes and
819 dredging-induced tidal prism changes: Mason Inlet, North Carolina. Journal of Coastal
820 Research 19, 1018-1025.
821 Costas, S. and FitzGerald, D., 2011. Sedimentary architecture of a spit-end (Salisbury Beach,
822 Massachusetts): The imprints of sea-level rise and inlet dynamics. Marine Geology 284, 203-
823 216.
824 Davis, R.A., Jr., Barnard, P., 2003. Morphodynamics of the barrier-inlet system, west-central
825 Florida. Marine Geology 200, 77-101.
826 Dillon, W.P., 1970. Submergence effects on a Rhode Island barrier and lagoon and inference on
827 barrier migration. Journal of Geology 78, 94-106.
828 Donnelly, J.P., 2006. A revised late Holocene sea-level record for northern Massachusetts, USA.
829 Journal of Coastal Research 22, 1051-1061.
830 Duffy, W., Belknap, D.F., Kelley, J.T., 1989. Morphology and Stratigraphy of Small Barrier-
831 Lagoon Systems in Maine. Marine Geology 88, 243-262.
832 Edwards, G.B., 1988. Late Quaternary geology of northeastern Massachusetts and Merrimack
833 Embayment, western Gulf of Maine. Unpublished M.S. Thesis, Boston University, Boston,
834 MA, 337 p.
835 Fairbanks, R.G., 1989. A 17,000 year glacio-eustatic sea level record: Influence of glacial
836 melting rates on the Younger Dryas event and deep-ocean circulation. Nature 342, 637-642.
837 FitzGerald, D.M., van Heteren, S., 1999. Classification of paraglacial barrier systems: coastal
838 New England, USA. Sedimentology 46, 1083-1108.

FitzGerald, D.M., Buynevich, I., and Argow, B., 2006. Model of tidal inlet and barrier island dynamics in a regime of accelerated sea level rise. Journal of Coastal Research, SI 39, 789-795.

FitzGerald, D.M., Buynevich, I.V., Davis, R.A., and Fenster, M.S., 2002. New England tidal inlets with special reference to riverine-associated systems. Geomorphology 48, 179-208.

FitzGerald, D.M., Buynevich, I.V., Hein, C.J., 2012. Morphodynamics and facies architecture of tidal inlets and tidal deltas, in: Davis, R.A., Dalrymple, R.W. (Eds.), Principles of tidal sedimentology. Springer, New York, 301-333.

FitzGerald, D.M., Kraus, N.C., Hands, E.B., 2001. Natural mechanisms for sediment bypassing at tidal inlets, U.S. Army Engineer Research and Development Center, Vicksburg, MS.ERDC/CHL CHETN-IV-30, 10 p.

FitzGerald, D.M., Penland, S., Nummedal, D., 1984. Control of barrier island shape by inlet sediment bypassing: East Frisian Islands, West Germany. Marine Geology 60, 355-376.

FitzGerald, D.M., Rosen, P.S., van Heteren, S., 1994. New England Barriers, in: Davis, R.A. (Ed.), Geology of Holocene Barrier Island Systems. Springer-Verlag, Berlin, pp. 305-394.

Folk, R.L. and Ward, W.C., 1957., Brazos River bar: a study in the significance of grain size parameters. Journal of Sedimentary Petrology 27, 3-26.

Forbes, D.L, 2005. Paraglacial Coasts, in: Schwartz, M.L. (Ed.), Encyclopedia of Coastal Science. Springer, Dordrect pp. 760-762.

Forbes, D.L., Orford, J.D., Carter, R.W.G., Shaw, J., Jennings, S.C., 1995. Morphodynamic evolution, self-organization, and instability of coarse-clastic barriers on paraglacial coasts. Marine Geology 126, 63-85.

861 Forbes, D.L., Syvitski, J.P.M., 1994. Paraglacial coasts, in: Carter, R.W.G., Woodroffe, C.D.
862 (Eds.), Coastal Evolution: Late Quaternary shoreline morph dynamics. Cambridge University
863 Press, Cambridge, 373-424.
864 Halsey, S.D., 1978. Late Quaternary Geologic History and Morphologic Development of the
865 Barrier Island System along the Delmarva Peninsula of the Mid-Atlantic Bight, Unpublished
866 Ph.D. dissertation, University of Delaware, 592 p.
867 Hayes, M. O., 1979. Barrier island morphology as a function of wave and tide regime, in:
868 Leatherman, S. P. (Ed.), Barrier islands from the Gulf of St. Lawrence to the Gulf of Mexico.
869 Academic Press, New York, NY, pp 1-29.
870 Hayes, M.O., Kana, T.W., 1976. Terrigenous clastic depositional environments: Some modern
871 examples. Technical report number 11-CRD, University of South Carolina, Coastal Research
872 Division, pp. 315.
873 Heaton, T.J., Blackwell, P.G., Buck, C.E., 2009. A Bayesian approach to the estimation of
874 radiocarbon calibration curves: the IntCal09 methodology. Radiocarbon 51, 1151–1164.
875 Hein, C.J., FitzGerald, D., Barnhardt, W., 2007. Holocene reworking of a sand sheet in the
876 Merrimack Embayment, Western Gulf of Maine. Journal of Coastal Research Special Issue
877 50, 863-867.
878 Hein, C.J., FitzGerald, D.M., Barnhardt, W.A., Stone, B.D., 2010, Onshore-offshore surficial
879 geologic map of theNewburyport East Quadrangle, Massachusetts, StateMap Preliminary
880 Map, 1 sheet.
881 Hubbard, D.K., 1971. Tidal inlet morphology and hydrodynamics of Merrimack Inlet,
882 Massachusetts. Unpublished M.S. Thesis, University of South Carolina, Columbia, SC, 144
883 p.

884 Imperato, D.P., Sexton, J.P., Hayes, M.O., 1988. Stratigraphy and sediment characteristic of a
885 mesotidal ebb-tidal delta, North Edisto inlet, South Carolina. Journal of Sedimentary
886 Petrology 58, 950-958.
887 Jarrett, J.T., 1976. Tidal prism-inlet area relationships, Vicksburg, Mississippi, U.S. Army Corps
888 of Engineers, GITI Report No. 3, 54 p.
889 Kaye, C.A., 1961. Pleistocene stratigraphy of Boston, Massachusetts. United States Geological
890 Survey Professional Paper, 424-B, pp. 73-76.
891 Kaye, C.A., Barghoorn, E.S., 1964. Late Quaternary sea-level change and crustal rise at Boston,
892 Massachusetts, with a note on the autocompaction of peat. Geological Society of America
893 Bulletin 75, 63-80.
894 Keene, H.W., 1971. Post glacial submergence and salt marsh evolution in New Hampshire.
895 Maritime Sediments 7, 64-68.
896 Kelley, J.T., 1987. Sedimentary environments along Maine's estuarine coastline, in FitzGerald,
897 D.M., Rosen, P.S. (Eds.), Glaciated Coasts. Academic Press, San Diego, pp. 151-176.
898 Kelley, J.T., 1995. The geological value of beaches as recreational environments and natural
899 habitats: An assessment of what is important and why, in: Colgan, C.S., (Ed.), Sustaining
900 Coastal Resources: Economics and Natural Sciences. Edmund S. Muskee Institute of Public
901 Affairs, University of Southern Maine, pp. 171-184.
902 Kelley, J.T., Dickson, S.M., Belknap, D.F., Stuckenrath, R., Jr., 1992. Sea-level change and late
903 Quaternary sediment accumulation on the southern Maine inner continental shelf, in:
904 Fletcher, C., Wehmiller, J. (Eds.), Quaternary coasts of the United States: Marine and
905 lacustrine systems. Society for Sedimentary Geology Special Publication 48, pp. 23-34.

906 Koteff, C., 1970. Surficial geologic map of the Milford quadrangle, Hillsborough County, New
907 Hampshire. U .S. Geological Survey Geologic Quadrangle Map GQ-881, scale 1:62,500.
908 Koteff, C., Robinson, G.R., Goldsmith, R., Thompson, W.B., 1993. Delayed postglacial uplift
909 and synglacial sea levels in coastal central New England. Quaternary Research 40, 46-54.
910 Kulp, M.A., FitzGerald, D.M., Penland, S., Motti, J., Brown, M., Flocks, J., Miner, M., McCarty,
911 P., Mobley, C., 2006. Stratigraphic Architecture of a Transgressive Tidal Inlet-Flood Tidal
912 Delta System: Raccoon Pass, Louisiana. Journal of Coastal Research Special Issue 39, 1731-
913 1736.
914 Kulp, M.A., Miner, M.D., FitzGerald, D.M., 2007. Subsurface Controls on Transgressive Tidal
915 Inlet Retreat Pathways, Mississippi River Delta Plain. Journal of Coastal Research Special
916 Issue 50, 816-820.
917 Levin, D.R., 1995. Occupation of a relict distributary system by a new tidal inlet, Quatre Bayou
918 Pass, Louisiana, in: Flemming, B.W., Bartholoma, A. (Eds.), Tidal signature in modern and
919 ancient sediments. International Association of Sedimentologists Special Publication 24, pp.
920 71-84.
921 McBride, R.A., Moslow, T.F., Roberts, H.H., Diecchio, R.J., 2004. Late Quaternary geology of
922 the northeastern Gulf of Mexico shelf: Sedimentary, depositional history, and ancient analogs
923 of a major shelf sand sheet of the modern transgressive systems tract, in: Anderson, J.B.,
924 Fillon, F.H. (Eds.), Late Quaternary Stratigraphic Evolution of the Northern Gulf of Mexico
925 Margin. Society of Sedimentary Geology Special Publication 79, Tulsa, pp. 55-83.
926 McCormick, C.L., 1969. Holocene stratigraphy of the marshes at Plum Island, Massachusetts.
927 Unpublished Ph.D. Thesis, University of Massachusetts, 104 p.

928 McIntire, W.G. Morgan, J.P., 1964. Recent Geomorphic History of Plum Island, Massachusetts,
929 and Adjacent Coasts. Louisiana State University Press, Baton Rouge.
930 Morton, R.A. Donaldson, A.C., 1973. Sediment distribution and evolution of tidal deltas along a
931 tide-dominated shoreline, Washapreague, Virginia, Sedimentary Geology 10, 285-299.
932 Moslow, T.F., Herron, S.D., 1978. Relict inlets: Preservation and occurrence in the Holocene
933 stratigraphy of southern Core Banks, North Carolina. Journal of Sedimentary Petrology 48,
934 1275-1286.
935 Moslow, T.F., Tye, R.S., 1985. Recognition and characterization of Holocene tidal inlet
936 sequences. Marine Geology 63, 129-151.
937 Munsell Color, 2000, Munsell soil color chart: Baltimore, Md., 22 p.
938 Neal, A., 2004. Ground-penetration radar and its use in sedimentology: Principles, problems, and
939 progress. Earth Science Reviews 66, 261-330.
940 Oldale, R.N., Colman, S.M., Jones, G.A., 1993. Radiocarbon ages from two submerged
941 strandline features in the western Gulf of Maine and a sea-level curve for the northeastern
942 Massachusetts Coastal Region. Quaternary Research 40, 38-45.
943 Oldale, R.N., Wommack, L.E., Whitney, A.B., 1983. Evidence for a postglacial low relative sea-
944 level stand in the drowned delta of the Merrimack River, western Gulf of Maine. Quaternary
945 Research 19, 325-336.
946 Oost, A.P., 1995. Dynamics and Sedimentary Development of the Dutch Wadden Sea with
947 Emphasis on the Frisian Inlet. A Study of Barrier Islands, Ebb-Tidal Deltas, Inlets and
948 Drainage Basins, Ph.D. Thesis: Utrecht University, Utrecht, Geologica Ultraiectina 126, 454
949 p.

950 Orford, J.D., Carter, R.W.G., Jennings, S.C., 1996. Control domains and morphological phases
951 in gravel-dominated coastal barriers. Journal of Coastal Research 12, 589-605.
952 Redfield, A.C., 1967. Ontogeny of a salt marsh, in: Lauff, G.H. (Ed.), Estuaries, American
953 Association for the Advancement of Science. Washington, DC, pp. 108-114.
954 Redfield, A.C., 1972. Development of a New England salt marsh. Ecological Monographs 42,
955 201-237.
956 Reimer, P.J., Baillie, M.G.L., Bard, E., Bayliss, A., Beck, J.W., Blackwell, P.G., Bronk Ramsey,
957 C., Buck, C.E., Burr, G.S., Edwards, R.L., Friedrich, M., Grootes, P.M., Guilderson, T.P.,
958 Hajdas, I., Heaton, T.J., Hogg, A.G., Hughen, K.A., Kromer, B., McCormac, F.G., Manning,
959 S.W., Reimer, R.W., Richards, D.A., Southon, J.R., Talamo, S., Turney, C.S.M., van der
960 Plict, J., Weyhenmeyer, C.E., 2009. IntCal09 and Marine09 Radiocarbon Age Calibration
961 Curves, 0–50,000 Years cal BP. Radiocarbon 51, 1111–1150.
962 Rhodes, E.G., 1973. Pleistocene-Holocene Sediments Interpreted by Seismic Refraction and
963 Wash-Bore Sampling, Plum Island-Castle Neck, Massachusetts, Technical Memorandum. U.
964 S. Army Corps of Engineers, Coastal Engineering Research Center 40, pp. 75.
965 Ridge, J.C., 2004. The Quaternary glaciations of western New England with correlations to
966 surrounding areas, in: Ehlers, J., Gibbard, P.L. (Eds.), Quaternary Glaciations, Extent and
967 Chronology Part II: North America. Elsevier, Amsterdam, pp. 169-199.
968 Rieu, R., van Heteren, S., van der Spek, A.J.F., De Boer, P.L, 2005. Development and
969 Preservation of a Mid-Holocene Tidal-Channel Network Offshore the Western Netherlands.
970 Journal of Sedimentary Research 75, 409-419.

971 Rodriguez, A.B., Hamilton, M.D., Anderson, J.B., 2000. Facies and Evolution of the Modern
972 Brazos Delta, Texas: Wave Versus Flood Influence. Journal of Sedimentary Research 70,
973 283-295.
974 Sammel, E.A., 1963. Surficial geology of the Ipswich Quadrangle, Massachusetts: U.S.
975 Geological Survey Geological Quadrangle Map GQ-0189.
976 Sammel, E.A., 1967. Water Resources of the Parker and Rowley River Basins, Massachusetts:
977 U.S. Geological Survey Hydrologic Investigations Atlas HA-247, scale 1:24,000.
978 Simcox, A.C., 1992. Water resources of Massachusetts. U.S. Geological Survey Water-
979 Resources Investigations Report 90-4122, pp. 94.
980 Siringan, F.P., Anderson, J.B., 1993. Seismic facies, architecture, and evolution of the Bolivar
981 Roads tidal inlet/delta complex, east Texas Gulf Coast. Journal of Sedimentary Petrology 63,
982 794-808.
983 Smith, J.B., FitzGerald, D.M., 1994. Sediment transport patterns at the Essex River Inlet ebb
984 tidal delta, Massachusetts, U.S.A. Journal of Coastal Research, 10, 752-774.
985 Smith, Q.H.T., Heap, A.D., Nichol, S.L., 2010. Origin and Formation of an Estuarine Barrier
986 Island, Tapora Island, New Zealand. Journal of Coastal Research 26, 292-300.
987 Stone, B.D., Borns, H.W., Jr., 1986. Pleistocene glacial and interglacial stratigraphy of New
988 England, Long Island, and adjacent Georges Bank and Gulf of Maine, in: Sibrava, V.,
989 Bowen, D.Q., Richmond, G.M. (Eds.), Quaternary Glaciations in the Northern Hemisphere.
990 Quaternary Science Reviews 5, pp. 39-52.
991 Stone, B.D., Pepper, J.D., 1982. Topographic control of the deglaciation of eastern
992 Massachusetts, in: Larson, G.J., Stone, B.D. (Eds.), Late Wisconsin Glaciation of New
993 England. Kendall/Hunt, Dubuque, pp. 145-166.

994 Stone, B.D., Stone, J.R., DiGiacomo-Cohen, M.L., 2006. Surficial Geologic Map of the Salem-
995 Newburyport East-Wilmington-Rockport 16 Quadrangle Area in Northeast Massachusetts,
996 U.S. Geological Survey Open-File Report, 2006-1260-B.
997 Stone, B.D., Stone, J.R., McWeeney, L.J., 2004. Where the glacier met the sea: Late Quaternary
998 geology of the northeast coast of Massachusetts from Cape Ann to Salisbury, in: Hanson, L.
999 (Ed.), New England Intercollegiate Geological Conference, Salem, Massachusetts, Trip B-3,
1000 25 p.
1001 Stone, J.R., Ashley, G.M., 1995. Timing and mechanisms of glacial Lake Hitchcock drainage.
1002 Geological Society of America Abstracts with Programs 27, 85.
1003 Stuiver, M. and Reimer, P.J., 1993. Extended 14C data base and revised CALIB 3.0 14C age
1004 calibration program. Radiocarbon 35, 215-230.
1005 Tye, R.S, 1984. Geomorphic Evolution and Stratigraphy of Price and Capers Inlets, South
1006 Carolina. Sedimentology 31, 655-674.
1007 Tye, R.S., Moslow, T.F., 1993. Tidal inlet reservoirs: Insights from modern examples, in:
1008 Rhodes, E.G., Moslow, T.F. (Eds.), Marine Clastic Reservoirs: Examples and Analogues.
1009 Springer, Berlin, pp. 77-99.
1010 Valentine, V., Hopkinson, C.S. Jr., 2005. NCALM LIDAR: Plum Island, Massachusetts, USA:
1011 18-19 April 2005. Elevation data and products produced by NSF-Supported National Center
1012 for Airborne Laser Mapping (NCALM) for Plum Island Ecosystems Long Term Ecological
1013 Research (PIE-LTER) Project. Final version. Woods Hole, MA: The Ecosystems Center,
1014 MBL.
1015 Vallino, J.J., Hopkinson, C.S., Jr., 1998. Estimation of dispersion and characteristic mixing times
1016 in Plum Island Sound estuary. Estuarine Coastal and Shelf Science 46, 333-350.

1017 Van Heteren, S., FitzGerald, D.M., McKinlay, P.A., Buynevich, I.V., 1998. Radar facies of
1018 paraglacial barrier systems: Coastal New England, USA. Sedimentology 45, 181-200.
1019 Vila-Concejo, A., Ferreira, Ó., Duarte, C., and Dias, J.M.A., 2003. The first two years of an
1020 inlet: sedimentary dynamics. Continental Shelf Research 23, 1425-1445.
1021 Zhao, L., Changsheng, C., Vallino, J., Hopkinson, C., Beardsley, R.C., Huichan, L., Lerczak, J.,
1022 2010. Wetland-estuarine-shelf interactions in the Plum Island Sound and Merrimack River in
1023 the Massachusetts coast. Journal of Geophysical Research 115, C1003

9. Figures and Tables

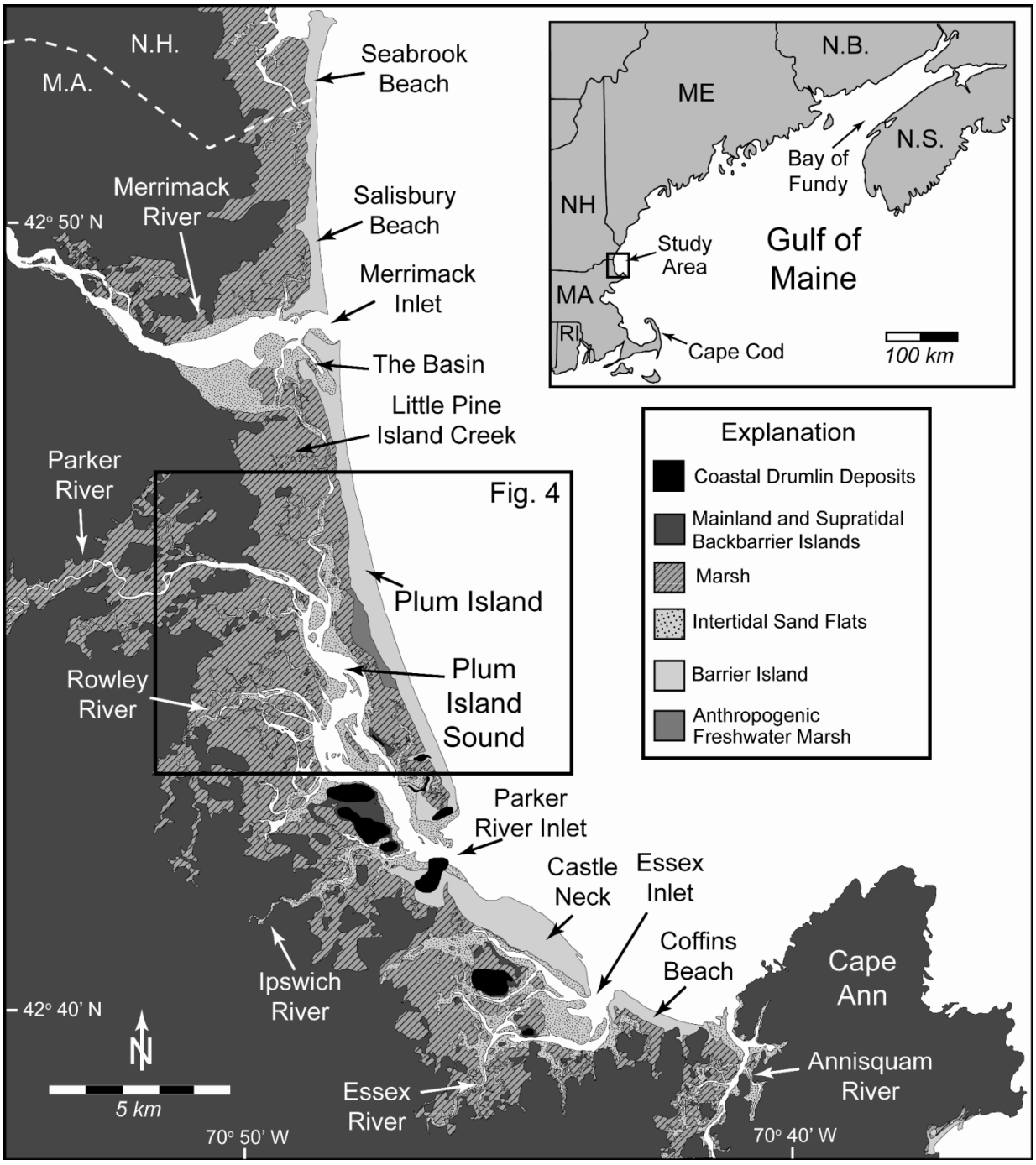

Figure 1. Study site map of Plum Island, located along the mixed-energy, tide-dominated coast of the Merrimack Embayment in northern Massachusetts, USA (western Gulf of Maine). It is bounded by the Merrimack River and Inlet to the north and the Parker River Inlet to the south, and backed by the extensive marsh and tidal flats of Plum Island Sound, into which the Parker, Rowley, and Ipswich Rivers drain. Map data from Stone et al. (2006) and this study.

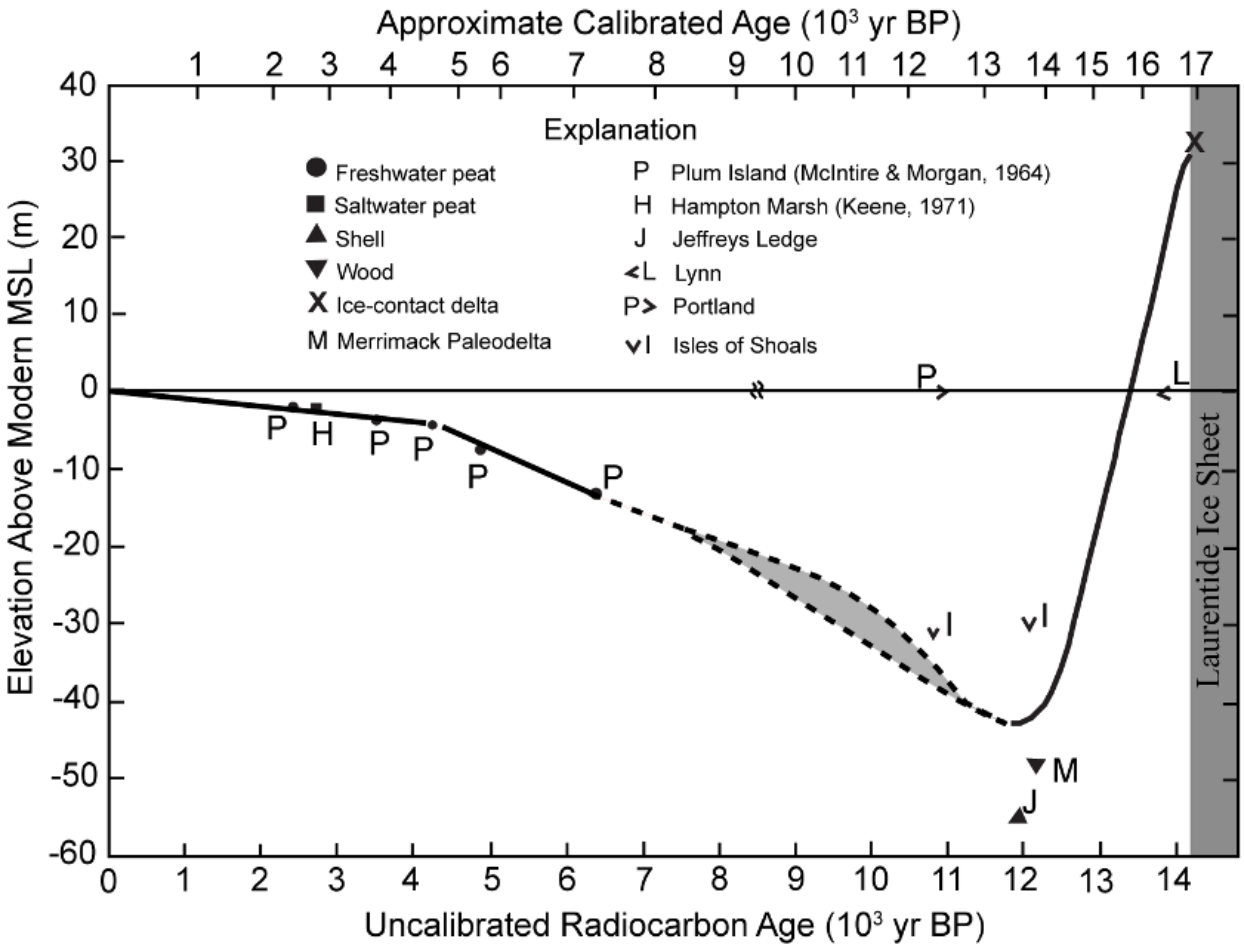

Figure 2. Relative sea-level curve for northeastern Massachusetts and adjacent inner continental shelf (calibrated radiocarbon dates provided in discussion in text). Calibrated age scale is approximate, based on calibrations given in Table 2. Vertical and temporal errors (uncertainties) are given by heights and widths of data rectangles. Modified from Oldale et al. (1993).

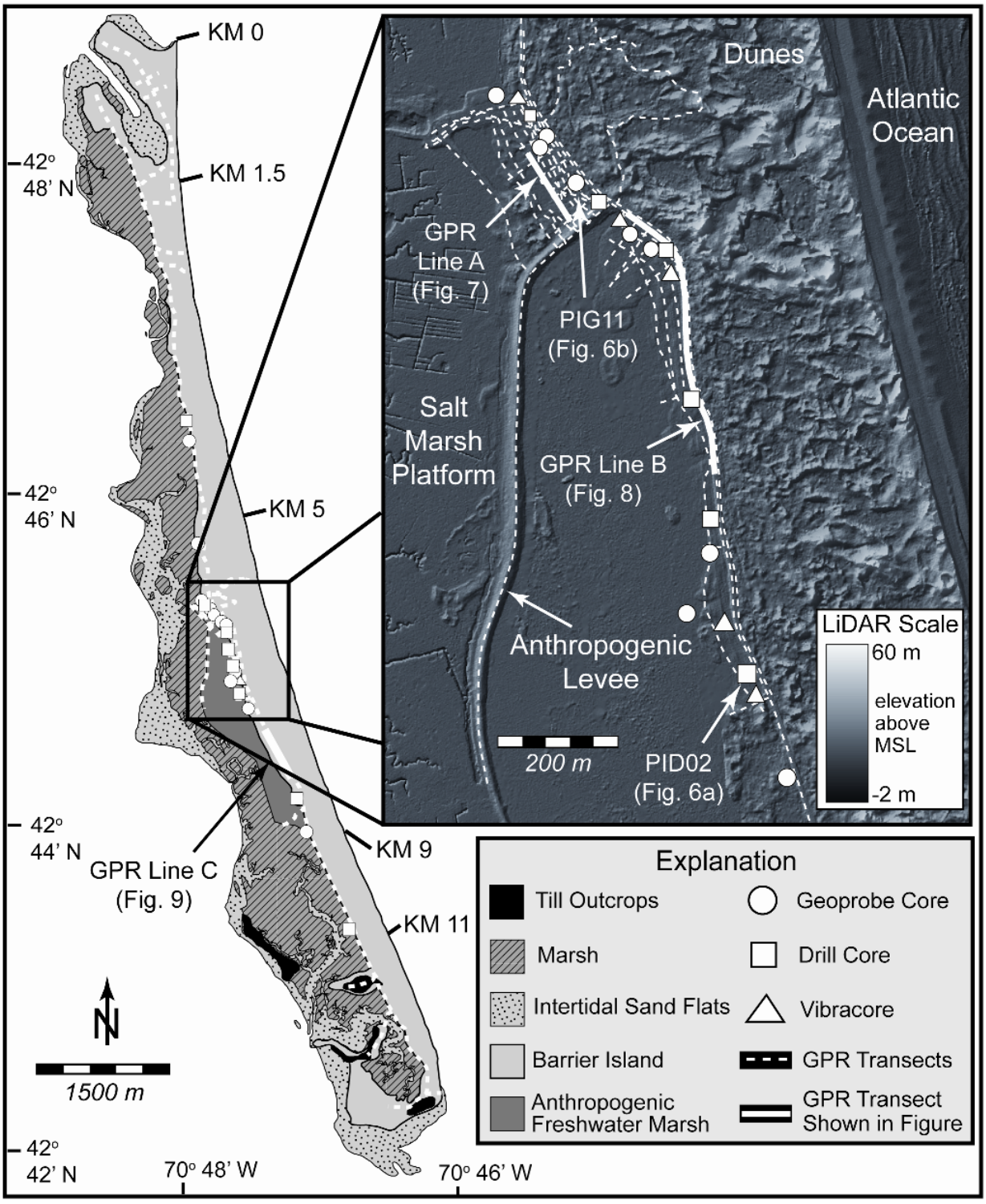

Figure 3. Map of data collection localities on Plum Island. Surficial map units are the same as in Fig. 1. Distance markers along Plum Island discussed in text are shown (KM 0, KM 1.5, etc). Inset map highlights data collected in central Plum Island, overlain on hill-shaded LiDAR data (Valentine and Hopkinson, 2005), shown for visualization purposes only (elevation range: -2 to 60 m MSL). Note locations of GPR transects shown in Figs. 7, 8, and 9, shown as thick solid lines in figure and inset.

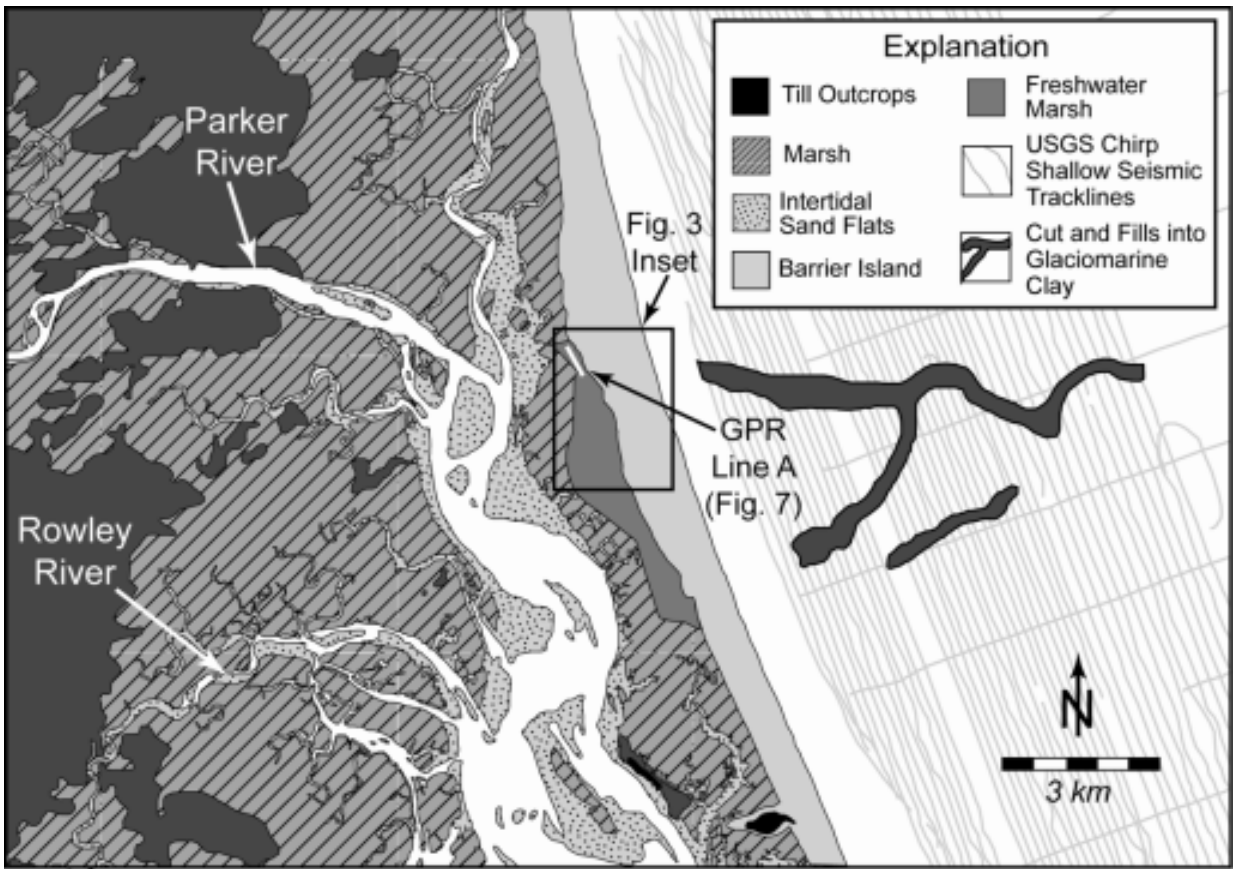

Figure 4. Spatial distribution of channel cut and fill features eroded into the glaciomarine clay buried offshore of central Plum Island, mapped in nearshore shallow seismic profiles. Shallow seismic profiles were collected using an EdgeTech Geo-Star FSSB system and an SB-0512i towfish (0.5–12 kHz) with 75–100 m line spacing (Barnhardt et al., 2009). These features are aligned with the modern Parker and Rowley Rivers where GPR Line A (Fig. 7) and core PIG11 (Figs. 6, 7) reveal channel-lag deposits overlying eroded glaciomarine sediments of Unit II beneath Plum Island.

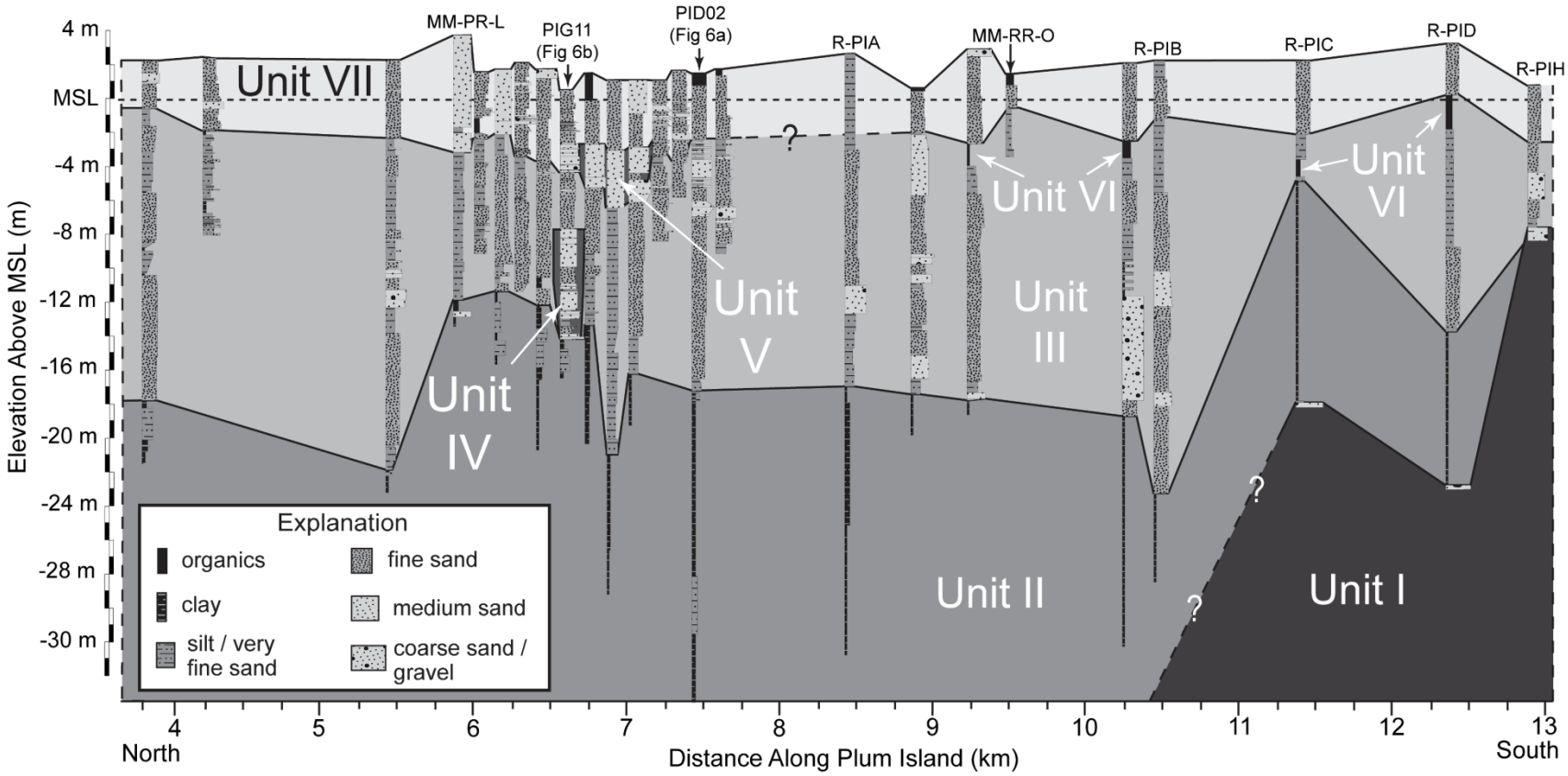

Figure 5. Shore-parallel stratigraphic cross section along the landward side of Plum Island, based on new (auger drill cores [PIDxx], and Geoprobe direct push cores, [PIGxx]; locations given in Fig. 3) and published cores. Horizontal scale corresponds to kilometer marks along Plum Island noted in Fig. 3. Cores labeled "PI" are new cores shown in Fig. 6. Cores labeled "MM-" are from McIntire and Morgan (1964). Cores labeled "R-" are from Rhodes (1973). Units are interpreted as: Unit I - till; Unit II – glaciomarine Presumpscot Formation; Unit III – backbarrier; Unit IV – fluvial channel fill; Unit V – inlet fill; Unit VI – saltwater peat; Unit VII – barrier spit.

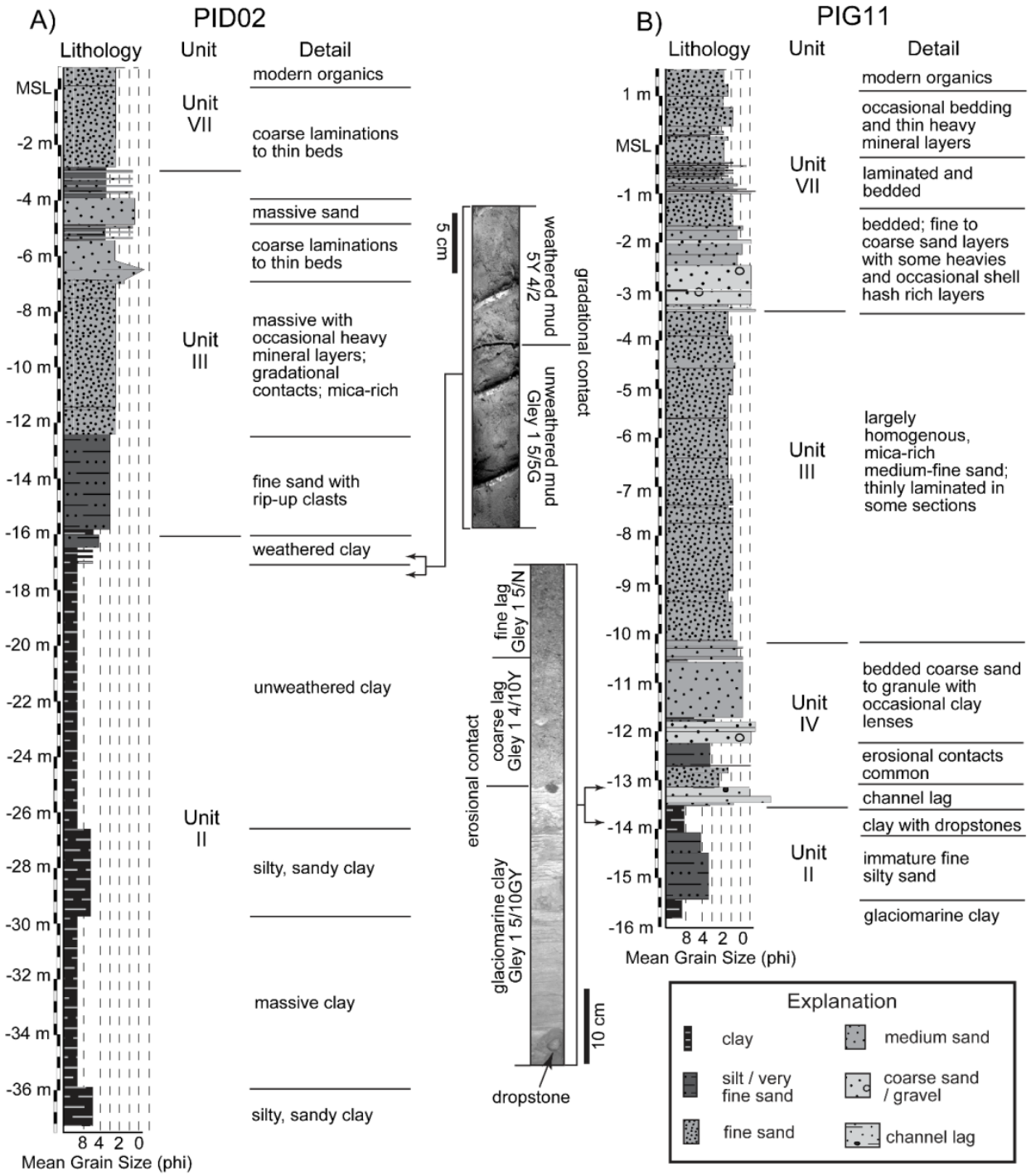

Figure 6. Logs from cores that penetrated through the barrier lithosome and into underlying glaciomarine clay units. Note different vertical scales. Insets are pictures from cores showing key contacts: weathered to unweathered glaciomarine clay in (A) and coarse gravel lag of the lowstand Parker River overlying erosional contact with glaciomarine clay in (B). Color notations associated with units in pictures after Munsell (2000). Units are interpreted as: Unit II – glaciomarine Presumpscot Formation; Unit III – backbarrier; Unit IV – fluvial channel fill; Unit VII – barrier spit. Core locations are shown in Fig. 3 and in context with other cores in Fig. 5.

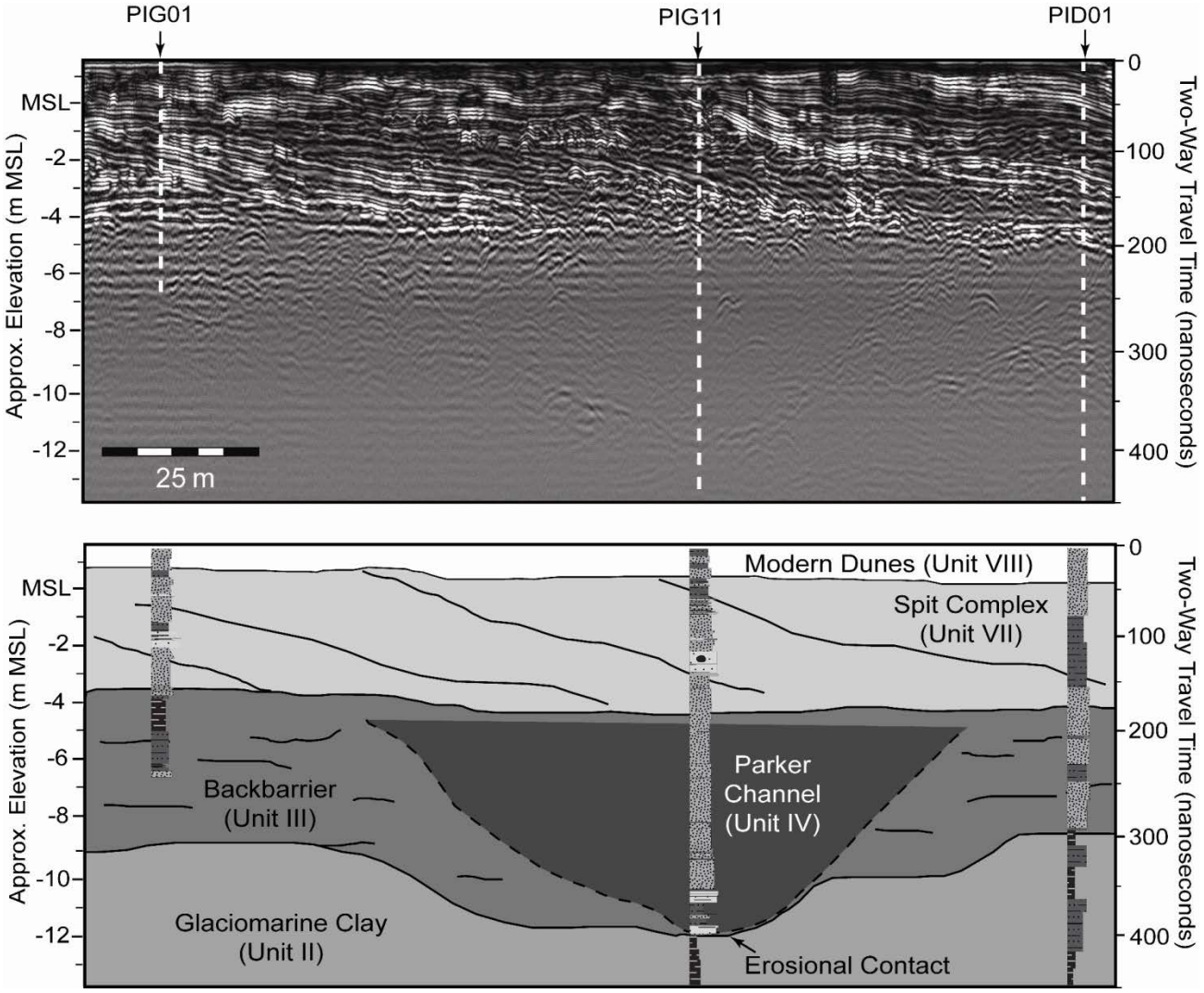

Figure 7. GPR Line A. Raw and interpreted shore-parallel GPR profile collected across lowstand Parker River channel with a Mala Pro-Ex with a 100 MHz antenna. TWTT: two-way travel time. Solid vertical white lines in upper image indicate locations of cores. Dashed lines indicate unit boundary designations shown in lower image. See Figs. 3 and 4 for location. For a high-resolution, uninterpreted version of GPR line, see Supplemental Fig. 1.

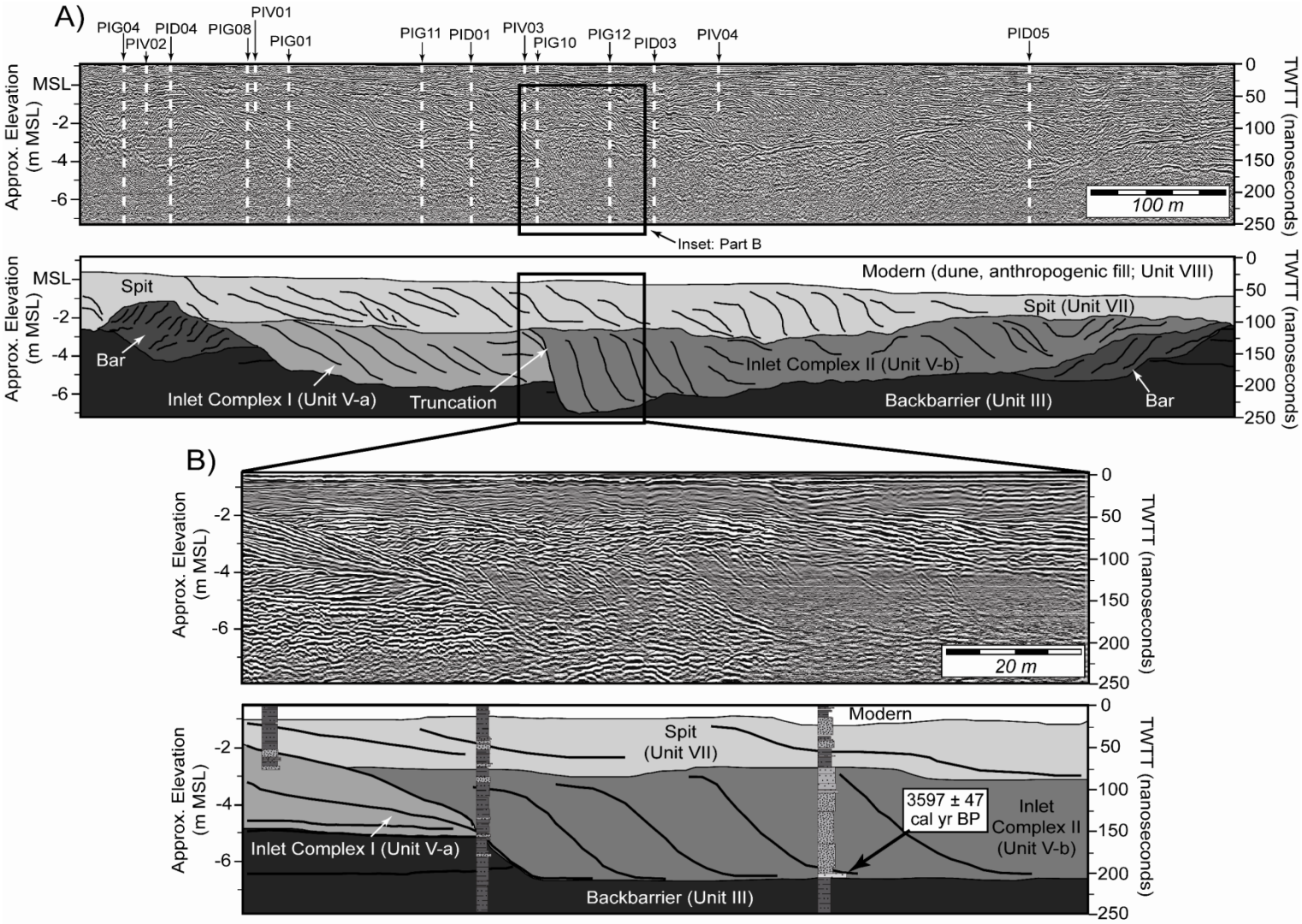

Figure 8. GPR Line B. Raw and interpreted shore-parallel GPR profiles collected across paleo-Parker Inlet sequence with a GSSI SIR2000 and a 200 MHz antenna. TWTT: two-way travel time. Solid vertical white lines in upper image indicate locations of cores. Dashed lines in upper images indicate unit boundary designations shown in lower image. See Fig. 3 for location. For a high-resolution, uninterpreted version of GPR line shown in (A), see Supplemental Fig. 2.

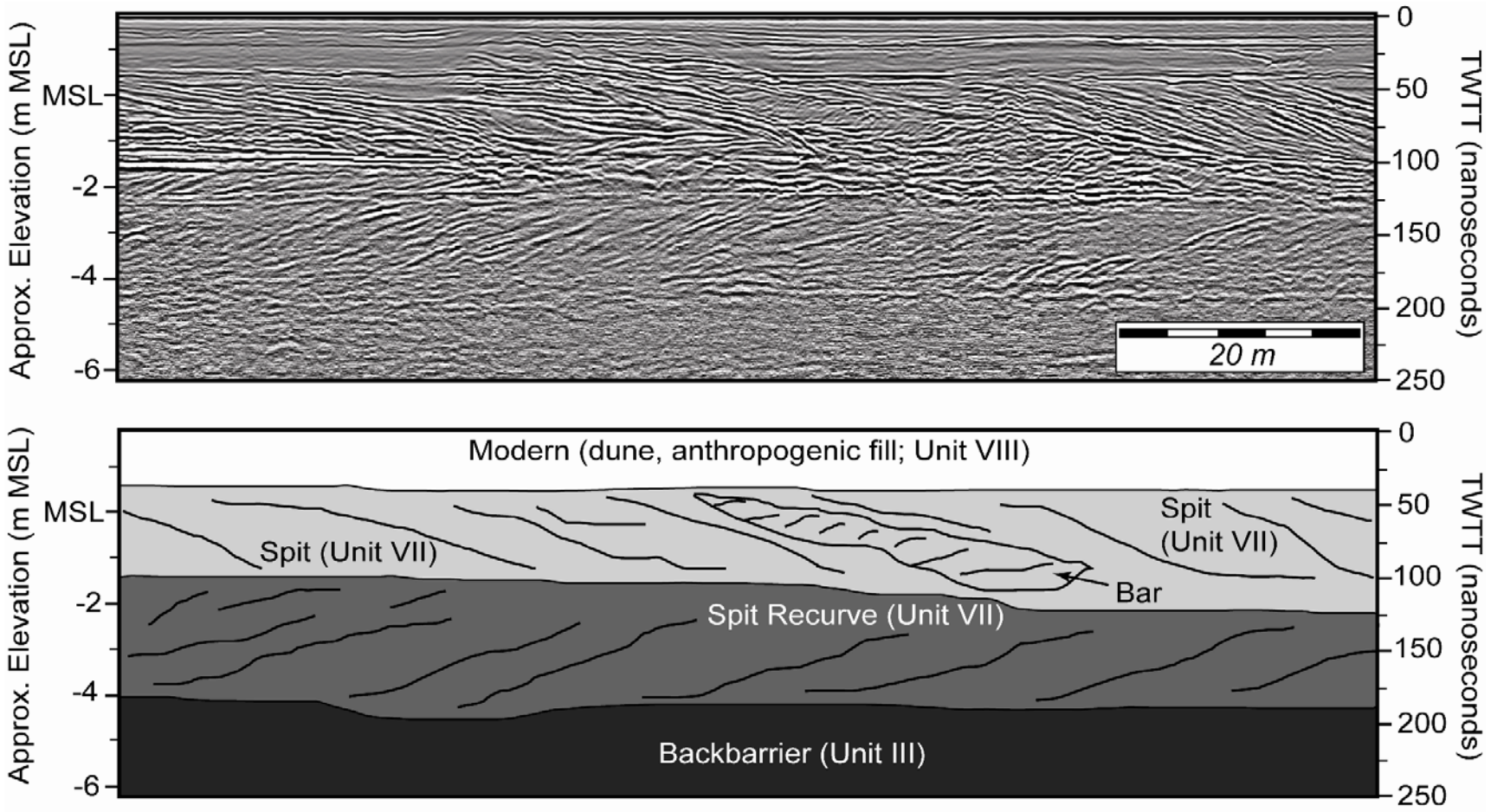

Figure 9. GPR Line C. Raw and interpreted shore-parallel GPR profiles collected across southerly spit sequence, south of paleo-Parker Inlet, with a GSSI SIR2000 and a 200 MHz antenna. Dashed lines in upper image indicate unit boundary designations shown in lower image. Note extensive northerly-dipping reflections overlying backbarrier sediment, interpreted as development of spit recurve. See Fig. 3 for location. For a high-resolution, uninterpreted version of GPR line in both grayscale and red-blue color, see Supplemental Fig. 3.

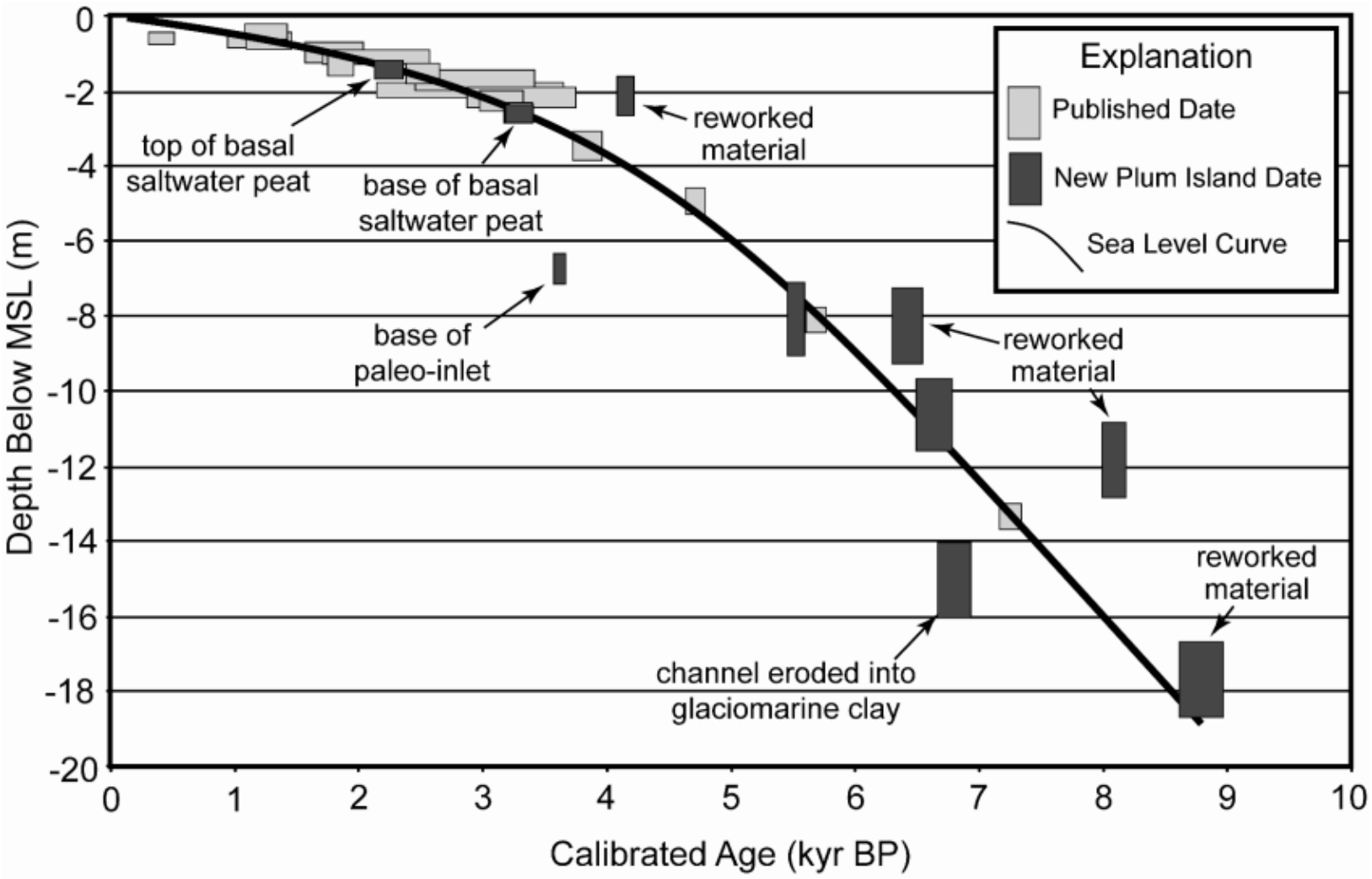

Figure 10. New dates from Plum Island (see Table 3) plotted on sea-level curve for northern Massachusetts based on dates presented by Donnelly (2006) and re-calibrated previously published dates, as given in Table 2. Vertical and temporal errors (uncertainties) are given by heights and widths of data rectangles. Due to the nature of the materials dated in this study (Table 3) and the problems with some of the older published sea level records (see Donnelly, 2006 for a complete discussion), these data are presented for comparison purposes only.

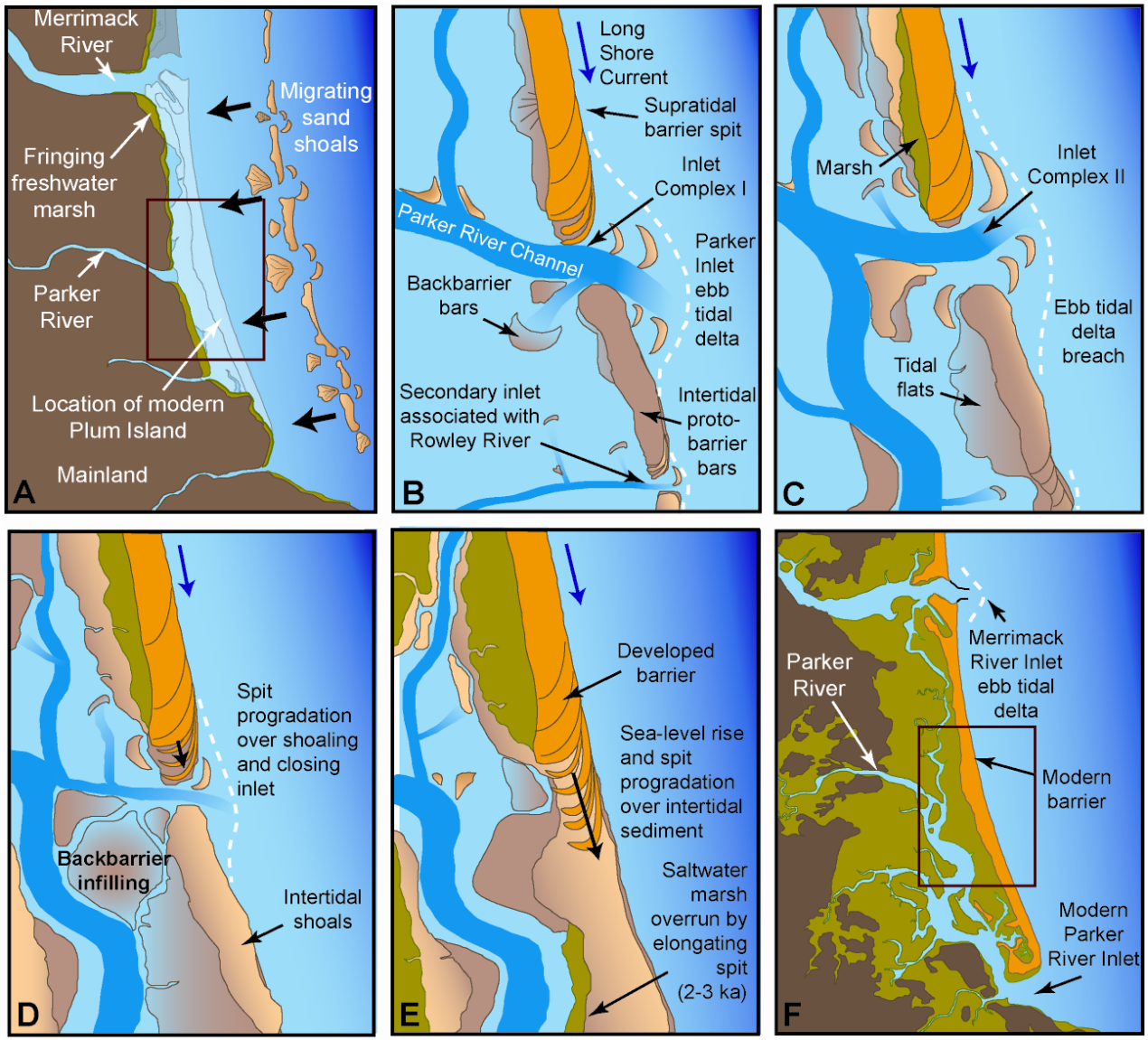

Figure 11. Evolutionary model for the formation of Plum Island. Note that views in B–E are within black box shown in A and F. (A) ***Transgressive Migration of Sand Shoals*** (13 to ~4 ka): regressive and lowstand deposits are reworked onshore during transgression;

Parker River maintains a course offshore of its present mouth, carving a channel into glaciomarine sediments; sands become pinned to glacial deposits as transgression proceeds; proto-barrier develops from continued sediment input initially without the development of a backbarrier. (B) ***Southerly Migration of Inlet*** (Prior to 3.6 ka): northeast storms produce southerly long shore transport (LST); island elongates by spit migration; paleo-Parker Inlet occupies Parker River channel and begins southerly migration. (C) ***Ebb Tidal Delta Breaching*** (~3.6 ka): Paleo-Parker Inlet deflected to north, truncating southerly prograding spit and platform; inlet narrows, deepens; backbarrier starts filling. (D) ***Closure of Inlet***: inlet shoals and narrows due to reduced tidal prism; LST causes southerly spit progradation and migration of 1–2 m deep inlet; increased backbarrier infilling. (E) ***Rapid Southerly Spit Progradation*** (3–2 ka): Paleo-Parker Inlet closes completely; spit rapidly progrades south, overtopping inlet fill sequences. (F) ***Barrier Island Stabilization*** (2 ka to Modern): Plum Island progrades with sediment from Merrimack River; Parker River joins Rowley and Ipswich Rivers as a single estuary with one inlet at the southern end of Plum Island, stabilized between two drumlins (Parker Inlet).

Table 1. Rivers of the Plum Island Backbarrier. Data compiled from Sammel (1967) and Simcox (1992). See Fig. 1 for locations.

River System	Inlet	Watershed Area, km^2	Annual Freshwater Discharge, km^3
Merrimack River	Merrimack	12885	6.24
Parker River	Plum Island Sound	167	0.033
Rowley River	Plum Island Sound	36	negligible (tidal)
Ipswich River	Plum Island Sound	402	0.056

Table 2. Recalibration of published radiocarbon dates from northern Massachusetts and southern New Hampshire. All dates were re-calibrated using Calib 6.0.1 (in conjunction with Stuiver and Reimer, 1993). Mixed and terrestrial samples (peat and organic matter) were calibrated with IntCal09 (Heaton et al., 2009) calibration curves. Marine samples (all mollusks) were calibrated using Marine09 (Reimer et al., 2009), corrected to a regional-averaged ΔR of 107 ± 37 years. All dates discussed in text are reported as 2-sigma calibrated ages before present (1950 AD).

Sample Location	Cited Sample ID	Reported Material Dated	Elevation (m MSL)	Reported Age (yrs BP)	Cal. 1-σ age (yrs BP)	Prob-ability	Cal. 2-σ age (yrs BP)	Prob-ability	Data Source
West Lynn, MA	W-735	barnacles (Balanus *hameri*)	1.6	14250 ± 250	16848 ± 311	1.000	16712 ± 845 15700 ± 23	0.995 0.005	Kaye and Barghoorn, 1964
Merrimack River Paleodelta (Offshore Plum Island)	NHAT-4	wood fragment	-48.0	12200 ± 80	14043 ± 125	1.000	14172 ± 365	1.000	Oldale et al., 1993
Jeffreys Ledge Paleo-barrier (Offshore Cape Ann)	MAAT-6	jackknife clam	-60.5	11900 ± 110	13253 ± 105	1.000	13273 ± 218 12995 ± 30	0.983 0.017	Oldale et al., 1993
Plum Island Backbarrier	PR-A	basal freshwater peat	-1.5	2450*	2465 ± 38 2667 ± 30 2392 ± 29 2604 ± 11 2534 ± 4	0.349 0.281 0.251 0.091 0.028	2488 ± 132 2670 ± 38	0.761 0.239	McIntire and Morgan, 1964
Plum Island Backbarrier	SR-L	basal freshwater peat	-3.5	3550*	3862 ± 42 3778 ± 17 3739 ± 14	0.640 0.203 0.157	3817 ± 118 3955 ± 17	0.931 0.069	McIntire and Morgan, 1964
Plum Island Backbarrier	PR-B-3	basal freshwater peat	-4.9	4225*	4730 ± 28 4830 ± 22 4661 ± 10	0.460 0.415 0.125	4689 ± 80 4824 ± 42 4591 ± 8	0.600 0.383 0.017	McIntire and Morgan, 1964
Plum Island Backbarrier	SR-K	basal freshwater peat	-8.1	4900*	5625 ± 36 5696 ± 2	0.987 0.013	5662 ± 80 5496 ± 8	0.980 0.020	McIntire and Morgan, 1964
Plum Island Barrier	PR-L	basal freshwater peat	-13.3	6280*	7213 ± 46	1.000	7234 ± 81 7071 ± 48	0.877 0.123	McIntire and Morgan, 1964
Hampton Marsh (Hampton, NH)**	I-4905	basal saltwater peat	-11.2	6850 ± 155	7709 ± 137	1.000	7709 ± 253 7446 ± 7	0.993 0.007	Keene, 1971
Hampton Marsh (Hampton, NH)**	I-4906	basal saltwater peat	-8.4	5730 ± 150	6535 ± 141 6357 ± 12 6328 ± 6	0.911 0.540 0.239	6583 ± 312 6227 ± 12	0.992 0.008	Keene, 1971

					6710 ± 2	0.011			
Hampton Marsh (Hampton, NH)	I-4908	basal saltwater peat	-2.0	2740 ± 310	2867 ± 385 2476 ± 5	0.992 0.008	2866 ± 752 3626 ± 2 2075 ± 1	0.999 < 0.001 < 0.001	Keene, 1971
Romney Marsh (Revere, MA)	R1	Juncus gerardi, Spartina patens	-2.56	3050 ± 50	3278 ± 65	1.000	3258 ± 118 3118 ± 9 3086 ± 6	0.967 0.018 0.016	Donnelly, 2006
Romney Marsh (Revere, MA)	R2	Distichlis spicata	-2.25	2950 ± 60	3135 ± 77 3037 ± 16 3010 ± 5	0.821 0.136 0.042	3310 ± 162 3307 ± 22	0.958 0.042	Donnelly, 2006
Romney Marsh (Revere, MA)	R3	Spartina patens	-1.83	2510 ± 50	2547 ± 54 2703 ± 24 2625 ± 16	0.589 0.238 0.173	2598 ± 147 2378 ± 12 2405 ± 7 2440 ± 4	0.948 0.029 0.014 0.008	Donnelly, 2006
Romney Marsh (Revere, MA)	R4	Juncus gerardi, Spartina patens, Scirpus spp.	-1.29	1900 ± 40	1855 ± 42 1748 ± 4 1916 ± 2	0.957 0.034 0.010	1827 ± 100	1.000	Donnelly, 2006
Romney Marsh (Revere, MA)	R5	Juncus gerardi, Spartina patens	-0.58	260 ± 50	305 ± 24 402 ± 28 161 ± 9 364 ± 5 3 ± 2	0.429 0.368 0.132 0.041 0.030	367 ± 100 180 ± 35 10 ± 11	0.769 0.184 0.467	Donnelly, 2006
Romney Marsh (Revere, MA)	R6	Spartina patens	-0.68	1040 ± 40	952 ± 28 1042 ± 3	0.966 0.034	982 ± 75 839 ± 7 805 ± 1	0.980 0.018 0.002	Donnelly, 2006
Neponset River Marsh (Milton, MA)	I-2275	high marsh saltwater peat	-0.37	1310 ± 95	1238 ± 71 1149 ± 14 1099 ± 8	0.838 0.106 0.056	1219 ± 168 1015 ± 18 991 ± 2	0.971 0.027 0.002	Redfield, 1967
Neponset River Marsh (Milton, MA)	I-2216	high marsh saltwater peat	-0.67	1360 ± 105	1276 ± 102	1.000	1240 ± 184 1487 ± 30 1437 ± 8 1020 ± 3	0.950 0.040 0.008 0.003	Redfield, 1967
Neponset River Marsh (Milton, MA)	I-2217	high marsh saltwater peat	-0.98	1860 ± 100	1797 ± 104 1641 ± 8 1917 ± 6	0.923 0.044 0.032	1773 ± 231 2031 ± 2	0.998 0.002	Redfield, 1967

Neponset River Marsh (Milton, MA)	W-1451	high marsh saltwater peat	-1.1	2100 ± 200	2104 ± 234	1.000	2075 ± 467 2667 ± 32 2602 ± 14 2566 ± 1	0.971 0.021 0.008 < 0.001	Redfield, 1967
Neponset River Marsh (Milton, MA)	W-1452	high marsh saltwater peat	-1.71	2790 ± 200	2976 ± 242 3235 ± 1	0.996 0.004	2907 ± 473 2379 ± 14 2405 ± 8	0.985 0.009 0.005	Redfield, 1967
Neponset River Marsh (Milton, MA)	W-1453	high marsh saltwater peat	-2.19	3110 ± 200	3312 ± 249 3044 ± 3	0.993 0.007	3284 ± 444 2811 ± 18 3808 ± 15 3757 ± 8	0.976 0.010 0.009 0.004	Redfield, 1967

* - no lab error reported in published literature; standard error of ± 50 applied in calibration

** - not used in construction of Holocene sea-level curve (Fig. 9), for reasons stated in Oldale et al., 1993

1109

Table 3. Results of ten radiocarbon analyses (accelerator mass spectrometry, AMS) of samples collected at Plum Island, MA for this study. Sample IDs given by core name: PIG – Geoprobe direct push core; PID – auger drill core. Core elevations were extracted from 2003 Mass GIS Digital Terrain Model data. Samples were submitted for radiocarbon analysis to either Beta Analytic Inc (Miami, FL, USA) or the National Ocean Sciences Accelerator Mass Spectrometry Facility (NOSAMS; Woods Hole, MA, USA). All dates are calibrated using Calib 6.0.1 (in conjunction with Stuiver and Reimer, 1993). Mixed and terrestrial samples (peat and organic matter) were calibrated with IntCal09 (Heaton et al., 2009) calibration curves. Marine samples (all mollusks) were calibrated using Marine09 (Reimer et al., 2009), corrected to a regional-averaged ΔR of 107 ± 37 years. All dates discussed in text are reported as 2-sigma calibrated ages before present (1950 AD).

Core / Sample ID	Lab ID	Latitude	Longitude	Depth Below MSL (m)	Straigraphic Unit	Dated Material	Reported Age (yrs BP)	Cal. 1-σ age (yrs BP)	Prob-ability	Cal. 2-σ age (yrs BP)	Prob-ability
PID03-S09	Beta: 240211	42.75452	-70.80078	8.3	Unit III (Backbarrier)	bivalve fragment	6090 ± 40	6385 ± 65	1.000	6402 ± 124	1.000
PID03-S13	Beta: 240212	42.75452	-70.80078	10.6	Unit III (Backbarrier)	bivalve fragment	6290 ± 40	6621 ± 73	1.000	6616 ± 141	1.000
PID03-S19	Beta: 240213	42.75452	-70.80078	11.6	Unit III (Backbarrier)	terrestrial wood fragment	7260 ± 40	8136 ± 21 8038 ± 20 8102 ± 13	0.393 0.383 0.224	8085 ± 87	1.000
PID04-S05	Beta: 240214	42.75669	-70.80397	8.1	Unit III (Backbarrier)	terrestrial wood fragment	4740 ± 70	5543 ± 41 5353 ± 23 5472 ± 17	0.517 0.275 0.208	5513 ± 81 5372 ± 53	0.646 0.354
PID05-S15	NOSAMS: 66043	42.75202	-70.80003	17.7	Unit III (Backbarrier)	bivalve fragment	8350 ± 30	8783 ± 103	1.000	8781 ± 171	1.000
PID11-S28	NOSAMS: 78101	42.73213	-70.78942	15.0	Unit III (Backbarrier)	bivalve fragment	6430 ± 40	6788 ± 72	1.000	6789 ± 138	1.000
PIG9-D5S3	NOSAMS: 72534	42.73215	-70.78942	1.5	Unit VI (saltwater peat)	basal saltwater peat (*in situ*)	2180 ± 40	2270 ± 35 2155 ± 29 2200 ± 1	0.581 0.408 0.011	2215 ± 112 2074 ± 11	0.967 0.033

PIG9-D5S12	NOSAMS: 72535	42.73215	-70.78942	2.6	Unit VI (saltwater peat)	bottom of basal saltwater peat (*in situ*)	3060 ± 35	3294 ± 47	1.000	3286 ± 79 3175 ± 9	0.975 0.025
PIG11-D04S04	NOSAMS: 78592	42.75556	-70.80286	2.1	Unit VII (Barrier Spit)	peat fragments (reworked)	3750 ± 35	4117 ± 37 4019 ± 16 4212 ± 2	0.772 0.211 0.017	4121 ± 61 4019 ± 34 4215 ± 18	0.654 0.243 0.103
PIG12-D07S08	NOSAMS: 78462	42.75434	-70.80108	6.7	Unit V (paleo-Parker Inlet)	muddy organics	3350 ± 30	3598 ± 40	1.000	3597 ± 47 3511 ± 31 3673 ± 12	0.745 0.195 0.060

1118

1119

Table 4. Inlet dimensions and equivalent tidal prisms of three modern inlets (Merrimack, Parker, and Essex) and one former (paleo-Parker) inlet of the southern Merrimack Embayment. Tidal prisms were calculated from cross-sectional areas using Jarrett's relationship for U.S. Atlantic inlets with one or zero jetties (Jarrett, 1976).

Inlet	Cross-Sectional Area, m^2	Equivalent Tidal Prism, m^3	Cross Sectional Area Data Source
Merrimack Inlet	1900	25.5×10^6	Hubbard, 1971
Parker Inlet	2500	32.9×10^6**	FitzGerald et al., 2002
Essex Inlet	1720	23.2×10^6	FitzGerald et al., 2002
paleo-Parker Inlet	2800	36.6×10^6	This study

** - Vallino and Hopkinson (1998) report a tidal prism of 32×10^6 m^3